SANDIA REPORT

SAND2008-6740
Unlimited Release
Printed October 2008

The Sandia MEMS Passive Shock Sensor: FY08 Testing for Functionality, Model Validation, and Technology Readiness

David S. Epp, Jill Blecke, Matthew R. Brake, Michael S. Baker, Jonathan W. Wittwer, Rebecca C. Clemens, John A. Mitchell, Jeremy A. Walraven

Prepared by
Sandia National Laboratories
Albuquerque, New Mexico 87185 and Livermore, California 94550

Sandia is a multiprogram laboratory operated by Sandia Corporation,
a Lockheed Martin Company, for the United States Department of Energy's
National Nuclear Security Administration under Contract DE-AC04-94AL85000.

Issued by Sandia National Laboratories, operated for the United States Department of Energy by Sandia Corporation.

Available to DOE and DOE contractors from
U.S. Department of Energy
Office of Scientific and Technical Information
P.O. Box 62
Oak Ridge, TN 37831

Telephone: (865) 576-8401
Facsimile: (865) 576-5728
E-Mail: reports@adonis.osti.gov
Online ordering: http://www.osti.gov/bridge

Available to the public from
U.S. Department of Commerce
National Technical Information Service
5285 Port Royal Rd.
Springfield, VA 22161

Telephone: (800) 553-6847
Facsimile: (703) 605-6900
E-Mail: orders@ntis.fedworld.gov
Online order: http://www.ntis.gov/help/ordermethods.asp?loc=7-4-0#online

SAND2008-6740
Unlimited Release
Printed October 2008

The Sandia MEMS Passive Shock Sensor: FY08 Testing for Functionality, Model Validation, and Technology Readiness

David S. Epp, Jill Blecke, Matthew R. Brake
Applied Mechanics

Michael S. Baker, Jonathan W. Wittwer
MEMS technologies

Rebecca C. Clemens, John A. Mitchell
Electromechanical Engineering

Jeremy A. Walraven
Microsystems Failure Analysis

Sandia National Laboratories
P.O. Box 5800
Albuquerque, New Mexico 87185-MS1070

Abstract

This report summarizes the functional, model validation, and technology readiness testing of the Sandia MEMS Passive Shock Sensor in FY08. Functional testing of a large number of revision 4 parts showed robust and consistent performance. Model validation testing helped tune the models to match data well and identified several areas for future investigation related to high frequency sensitivity and thermal effects. Finally, technology readiness testing demonstrated the integrated elements of the sensor under realistic environments.

Acknowledgments

The authors gratefully acknowledge funding and support from the Embedded Evaluation program run by Bob Paulsen and Paul Yoon, the Campaign 6 program run by T.Y. Chu, the Campaign 5 program run by Davina Kwon, the DSW Campaign run by Mike Sjulin and Russ Miller, and the overall support and guidance of Mary Gonzales. Without this support the accomplishments documented here would have not been possible.

The authors would also like to thank Brandan Rogillio and Doug Van Gothem from the Mechanical Shock Lab, Brian Resor, Danny Gregory, and Ron Coleman from the Mechanical Vibration Lab, and Sarah Leming from the Climatic Lab for their help in accomplishing the large amount of testing in this report. Additionally, Ken Pohl, Jaime Stamps, and Jack Heister were instrumental in developing the suite of test fixturing, electronics, and software that made the testing possible.

Finally, special thanks go to Patricia Oliver for helping to create the form and legibility of the report.

Contents

Figures

Tables

Acronyms

Acronyms and Abbreviations

FFT	Fast Fourier Transform
CG	Center of gravity
LCC	Leadless chip carrier
LDV	Laser Doppler vibrometer
MEMS	Micro-electro-mechanical systems
MIL Specs	Military specifications
SUMMiT V™	Sandia ultra-planar, multi-level MEMS technology 5

1. Introduction

The Sandia Micro-electro-mechanical systems (MEMS) Passive Shock Sensor is intended to be a threshold acceleration sensor that latches an electrical contact into the closed position when it detects acceleration above its designed set point. No applied power is required to sense a shock event or to store that information for a single event. Power is required only to measure the open or closed state of the switch, or to reset the switch for continued sensing. A detailed description of the device, as well as information on the design, modeling, packaging, and testing is given in prior reports and papers [Mitchell et al., 2006, Wittwer et al., 2008a, Mitchell et al., 2008]. This report provides an overview of the FY08 testing activities focused on functionality, model validation, and technology readiness for the Sandia MEMS Passive Shock Sensor.

1.1 Background

The MEMS passive shock sensors are fabricated using the SUMMiT V™ surface micromachining process. Currently, there are seven design revisions, either fabricated or submitted for fabrication, for the passive shock sensor. An overview of the various revisions is given in the report covering the design and modeling for FY08 [Wittwer et al., 2008b]. The testing program in FY08 focused on design revision 4 almost exclusively. Revision 4 unpackaged dice were available very early in the year and packaged devices were available shortly thereafter. Three other revisions became available during the year but revision 4 remained the main priority for testing.

Revision 4 has four switches on each die, each with a different shock threshold. Figure 1 shows the die layout for revision 4. The four switches on each die are labeled J4A-D, J4C-D, J4B, and J4D in order of increasing threshold estimates based on early modeling. The direction of switch closure is also shown on the figure.

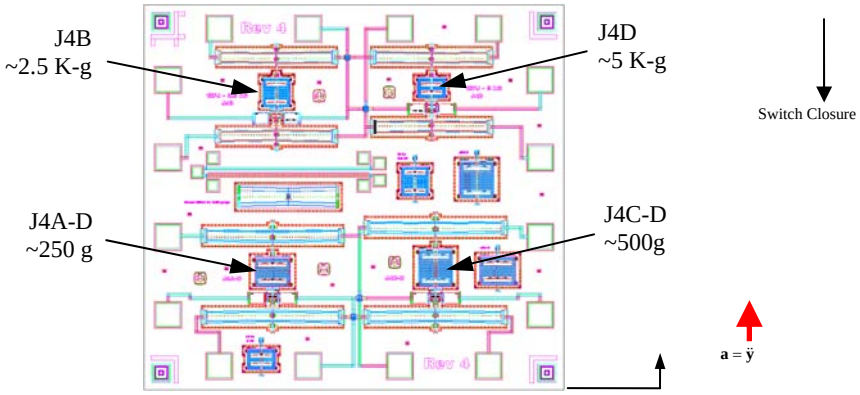

Figure 1. Revision 4 die layout showing four switches, each with a different threshold. Initial threshold estimates shown.

A pair of actuators allows each switch to be toggled open or closed. This allows for a self-test of the switch that is used extensively during testing to determine switch health. This self-test consists of an open command, close command, and open command—all run sequentially (in series). If the switch fails to respond to any of these commands it is deemed inoperable. A set of

test electronics and software is used to implement this self-test and to query the switch states after tests. This electronics and software is covered in more detail in the appendix.

For most of the testing presented in this report, the revision 4 die were packaged to facilitate testing. Figure 2 shows the current packaging process steps. For more detail on this process, refer to the report covering the FY08 packaging efforts [Baker et al., 2008]. The fixturing used for the testing is documented in the appendix.

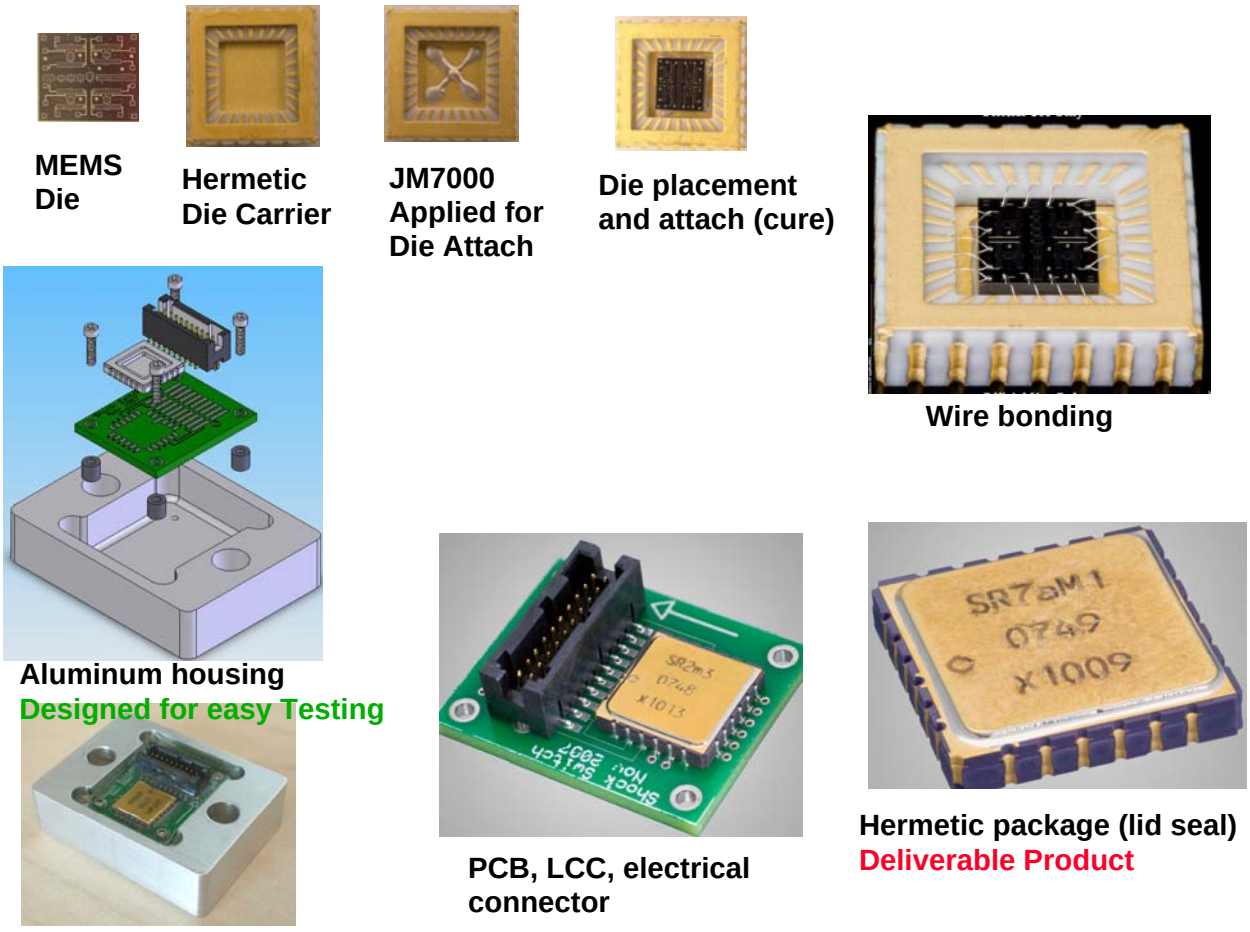

Figure 2. Current package cycle used for all revision 4 packaged parts tested.

During testing, parts were pulled from further testing and sent to failure analysis when they started to show consistent failures of the self-test. The goal was early identification of failure modes in order to effect subsequent design revisions. The details of those analyses are contained in the report detailing the FY08 failure analysis [Walraven et al., 2008].

The remainder of this report covers functionality testing, model validation, and technology readiness. Each test conducted is described in its own section along with results and a brief discussion of those results. Next, general conclusions are presented along with a discussion of future work. Finally, the appendix covers fixturing, electronics, and software used to facilitate the testing.

2. Functionality and Model Validation

The two main objectives of this testing are to verify functionality of the packaged Sandia MEMS Passive Shock Sensor and to provide data from fabricated parts to compare with the models of those parts for validation. Functionalities of critical interest are shock sensing and storage capability and the self-test. Both of these were verified with the first test series which simultaneously verified functionality and gathered data to compare to model predictions for switch shock thresholds. Other tests measured both thermal and mechanical properties of the devices for comparison with model predictions. Some discussion of the model results is included in each section. For full details of the modeling effort, refer to the FY08 report on the subject [Wittwer et al., 2008b].

2.1 Shock Threshold

2.1.1 Purpose

The goals of the shock threshold tests were to verify switch functionality and validate model predictions for shock threshold. Initial model predictions were available early in the design cycle for revision 4 and are shown in Figure 1. These initial predictions were updated as testing was in progress. Comparisons in the following results are with the most recently updated model predictions and are in good agreement.

2.1.2 Test Description

Most of this testing was done with fourteen parts, although initial testing at 5000 g's used only eight parts. Another seven parts became available directly after 5000 g shock level was completed so the total increased to fifteen for a few more tests. Finally, one part was removed for failure analysis due to device failures. Each packaged part was installed onto the shock fixture on one of three sides. Figure 3 shows the fully populated fixture with and without the cover clamp installed. Note that a part is defined as a fully packaged MEMS die as shown in the lower left image of Figure 2. A part has 4 devices as shown in Figure 1.

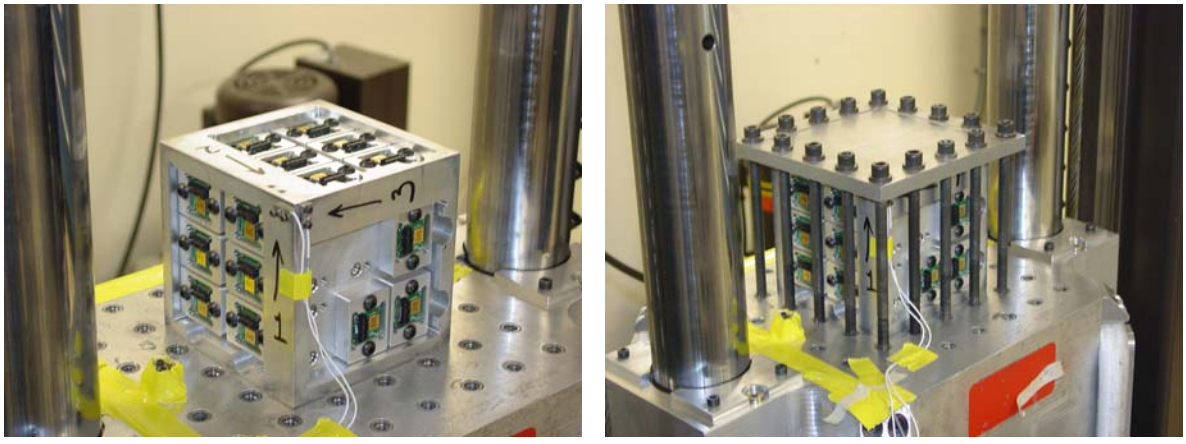

Figure 3. Initial functionality test parts installed on drop table fixture.

A large drop table was used to apply shocks to the parts. The fixture was clamped to the drop table carriage and accelerometers were installed in the two off-axes for data collection during the shock. Also, a control accelerometer was affixed to the carriage for the drop table. For each shock level, three drop events were needed corresponding to switch closure directions for each of the three faces of the fixture. This was accomplished by rotating the fixture between tests. Prior to each drop the switches were opened in preparation for sensing a shock. After each shock was applied, switch states were recorded and each switch was self-tested to verify functionality; then each switch was reset open for subsequent tests. Initially, the pulse width (see [Mitchell et al., 2008]) was specified to be less than 1 millisecond in length for all drops. Due to equipment limitations the actual shock amplitude experienced by the parts varied up to 15% from the desired values.

When testing began, switch closure results were very irregular and inconsistent with expectations. Through a long period of trial and error and discussions with the modeling team, it was concluded that switch sensitivity to high frequency inputs was the cause of these problems. Even though most of the shock energy was in the main pulse with frequency content well below the switch resonant frequencies, sufficient energy was contained in the higher frequencies to affect switch response. Some time was spent tuning drop tables to minimize higher frequency content shocks it was producing, but this was only marginally successful and produced intermittent results. The final solution that produced very consistent shock switch results was to use a much wider shock pulse duration (~2 ms) along with mechanical filtering at the fixture. The mechanical filtering was produced by two sheets of 0.25-in., 60 duro fluorosilicone, isolating the fixture from the carriage. The auxiliary accelerometer locations were moved closer to the location of packaged parts under test to increase measurement fidelity. Figure 4 shows the final setup used for the majority of functionality and threshold testing. Note the thin blue pads in right image of Figure 4.

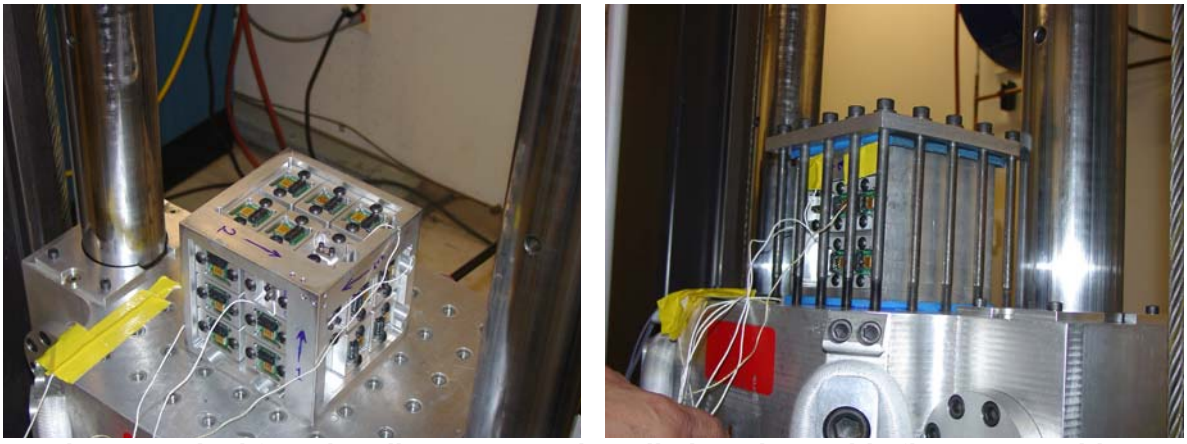

Figure 4. Final functionality test parts installed on drop table fixture. Note blue mechanical isolation material in right image.

2.1.3 Results

One of the major results from this testing was the increased attention to high frequency sensitivity of the shock switch devices. This motivated further testing and a large effort to mitigate and understand this phenomenon. Testing was conducted later in the year to study high frequency response directly and is covered in Section 2.6.

Once mechanical filtering was added to the test fixture, switch responses became very consistent. Figure 5 shows functionality test results for revision 4 parts that resulted from this test series. The vertical axis represents the fractional percentage of devices that closed for a given shock level (horizontal axis). Symbols correspond with a particular test; lines connecting symbols were drawn to improve legibility and distinguish individual device responses.

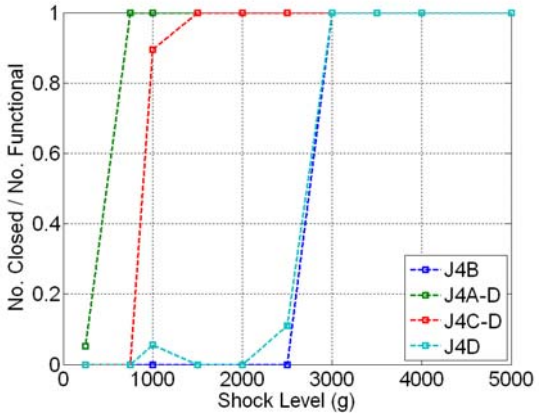

Figure 5. Functionality test results for revision 4 switches.

Table 1 is a low/high tabular representation of Figure 5; it also compares measured results with model predictions. The measured results show the range between a shock level that doesn't close any switches (low) and a shock level that closes all switches available (high). These model results were the most recent available at the time of this writing and reflect iterations from initial estimates for revision 4 shown in Figure 1 [Wittwer et al., 2008b]. These final results show very good agreement between measured results and the modeling results.

Table 1. Comparison of Measured and Modeled Results

	Measured Threshold Bounds		**Modeled Threshold Bounds 95% Confidence Level**	
Switch	**Low (g's)**	**High (g's)**	**Low (g's)**	**High (g's)**
J4A-D	250	750	329	406
J4C-D	750	1500	688	843
J4B	2500	3000	2517	3327
J4D	2000	3000	1638	5342

2.2 Thermal Sensitivity of Bi-stability

2.2.1 Purpose

The goal of the thermal sensitivity testing was to validate model prediction that no bi-stability (see [Mitchell et al., 2006, Mitchell et al., 2008]) loss would be observed at the normal environment temperature extremes [Skousen and Cap, 2007]. Also, some indication was desired of how packaging features affect bi-stability during exposure to thermal environments. Modeling predictions (see [Mitchell et al., 2008, Wittwer et al., 2008b]) indicated that device performance (quasi-static thresholds) would degrade at normal environment temperature extremes (165° to -65°F), with the most effect from the cold extreme. Modeling did not predict a loss of bi-stability at these temperatures [Wittwer et al., 2008b].

2.2.2 Test Description

Two sets of tests were run to verify thermal sensitivity with respect to bi-stability. The first was a test with bare die, metalized die, and die in leadless chip carrier (LCC) packages taken to three low temperature conditions of increasing severity. The second was a test with fully packaged switches taken 20°F above the hot normal environment temperature and 10°F below the cold normal environment temperature. Together these two tests span the packaging process (shown in Figure 2) from bare die to fully packaged switches. All this testing was conducted in thermally controlled climatic chambers.

2.2.2.1 Bare Dice, Metalized Dice and LCC Packaged Dice

Nine total parts were tested: three non-metalized dice, three metalized dice, and three dice packaged in LCCs. The parts were assembled on a flat aluminum plate to which a sensor was affixed to monitor the part temperature separate from the chamber temperature.

Since the models predicted cold temperatures to be most critical, three cold temperature levels were investigated: -30°F, -50°F, and -70°F. Before the first test, each part was set to the open position. The parts were then placed in the thermal chamber and ramped to the desired temperature level at a rate of less than 5°F per minute. The parts were allowed to soak in the chamber for 15 minutes before returning to room temperature. After each temperature-level test, all parts were removed, their sense mass positions were recorded, and they were reset to the open position. The dice and metalized dice were photographed between tests. The LCC packaged parts were self-tested using the test electronics.

2.2.2.2 Fully Packaged Parts

Eight fully packaged shock switch parts were tested. All of the parts were assembled onto the large test fixture made for shock and vibration testing (see appendix).

Before testing began, each part was self-tested to verify operability and to position sense mass in the open position. The test fixture was then placed into a thermal chamber and soaked at 185°F for one hour. Then the fixture was removed and each part was immediately self-tested again to determine switch state and verify operability; then switches were reset to the open position. Once parts were back to room temperature, they were placed in the thermal chamber again and soaked

at -75°F for 45 minutes. Once again, parts were removed and a self-test was performed. Finally, after the parts had returned to room temperature a final self-test was performed.

2.2.3 Results

2.2.3.1 Bare Dice, Metalized Dice and LCC Packaged Dice

All devices were checked for spontaneous closures after each temperature cycle. Spontaneous closures (closures not generated by inertial input to the switch) would indicate a loss of bi-stability at the temperature extreme. None of the devices tested showed spontaneous closures and therefore none showed a loss of bi-stability. This agreed with modeled results.

2.2.3.2 Fully Packaged Parts

All devices were checked for spontaneous closures after each temperature cycle. Similarly to the test described in Section 2.2.2.1 above, spontaneous closures (closures not generated by inertial input to the switch) would indicate a loss of bi-stability at the temperature extreme. Figure 6 shows the number of spontaneous closures after both the high and low temperature cycles. The high temperature test did not create any closures while the cold temperature test closed most of the J4A-D and J4C-D devices and one each of the J4B and J4D devices. This indicates that the -75°F temperature is well below the average temperature needed to produce spontaneous closures in the J4A-D and J4C-D devices while just barely cold enough to start spontaneously closing J4B and J4D devices. Figure 7 shows self-test results after each phase of the temperature cycle tests. A pretest check and a post test check, both at room temperature, are included. The most notable observation is that the self-test showed nonfunctional J4A-D and J4C-D devices when applied as quickly as possible after the parts came out of the thermal chamber. All of the J4B and J4C devices were still functional. Model predictions for thermal sensitivity did not include the aluminum housing package so there are no model/test comparisons for these results.

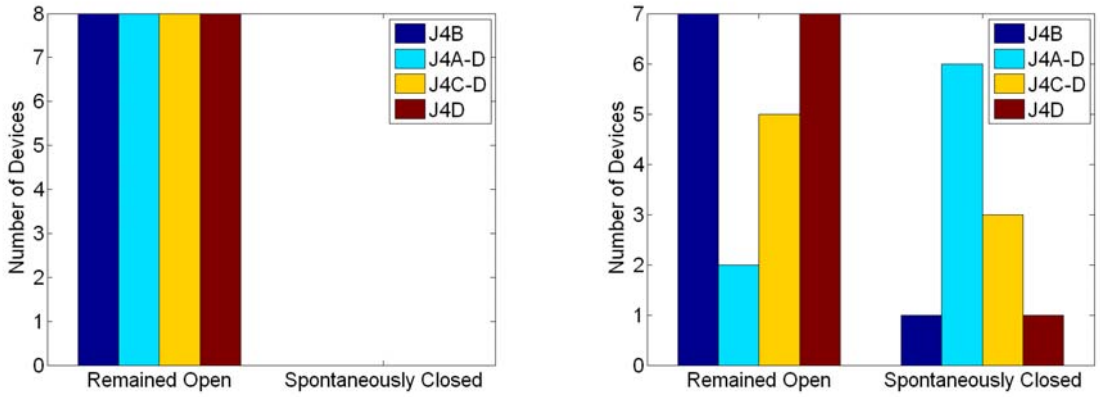

Figure 6. Spontaneous closures of fully packaged devices due to thermal exposure: (a) after 185°F for 1 hr and (b) after -75°F for 45 min.

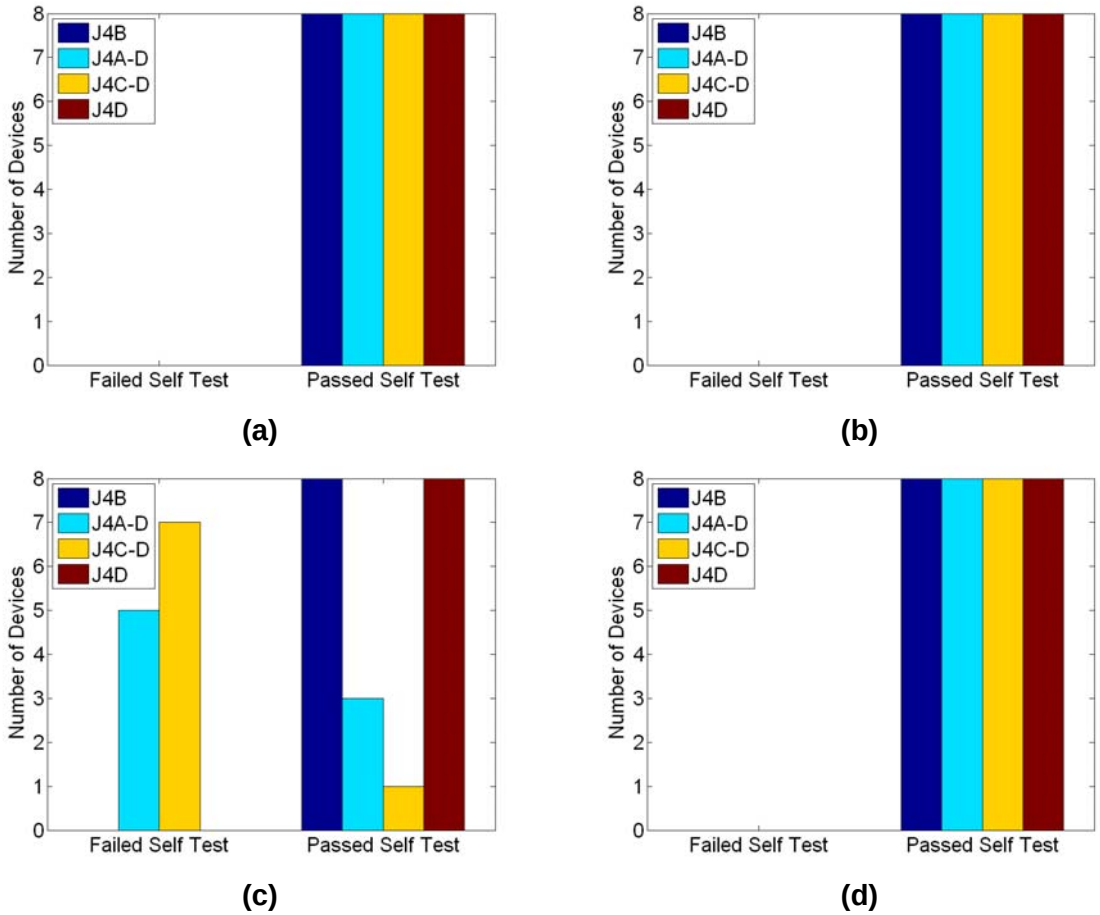

Figure 7. Self-test results for fully packaged devices: (a) before thermal environments, (b) after 185°F for 1 hr, (c) after -75°F for 45 min, (d) after returning to room temperature.

2.3 Thermal Sensitivity of Switch Threshold

2.3.1 Purpose

The goal of this testing was to determine switch threshold variations due to thermal extremes. Hardware limitations and loss of bi-stability discussed in the last section made it impossible to conduct drop table tests at cold temperatures so the focus was on threshold shift at the high temperature extreme of 165°F [Skousen and Cap, 2007]. Time limitations in the shock lab dictated that only a single threshold need be tested. Since both the J4B and J4D devices had thresholds around 2500 g's that shock level was the focus of testing. Model results were available for comparison but the measured data lacked the resolution needed for it.

2.3.2 Test Description

Five fully packaged parts (affixed to the shock fixture) were used for this test. The devices were shocked at ambient conditions to form a baseline for the later tests at hot conditions. Once baseline data was taken, the parts and fixture were heated in an oven to 185°F. Once they

reached this temperature, they were soaked for 1 hour then quickly removed from the oven, attached to the drop table, and shocked. Preparatory testing indicated that the large mass of the drop table fixture would cool to 165°F within 8-10 minutes of removal from an over at 185°F. All of the drop table shocks were applied within 5 minutes of removal from the oven.

2.3.3 Results

Figure 8 shows a comparison of the baseline and hot temperature shock test results. There are some obvious differences in results between the ambient and hot tests for these two switches, but it is not consistent. In the case of J4B, the threshold seems to have decreased and for J4D the threshold increased. Model results indicate that the threshold should have increased slightly at elevated temperatures. More tests are needed, including testing at cold temperatures, to fully understand the phenomenon and its effect on threshold. The one significant conclusion that can be taken from the data is that the switch threshold does not change significantly between ambient and the hot temperature extreme.

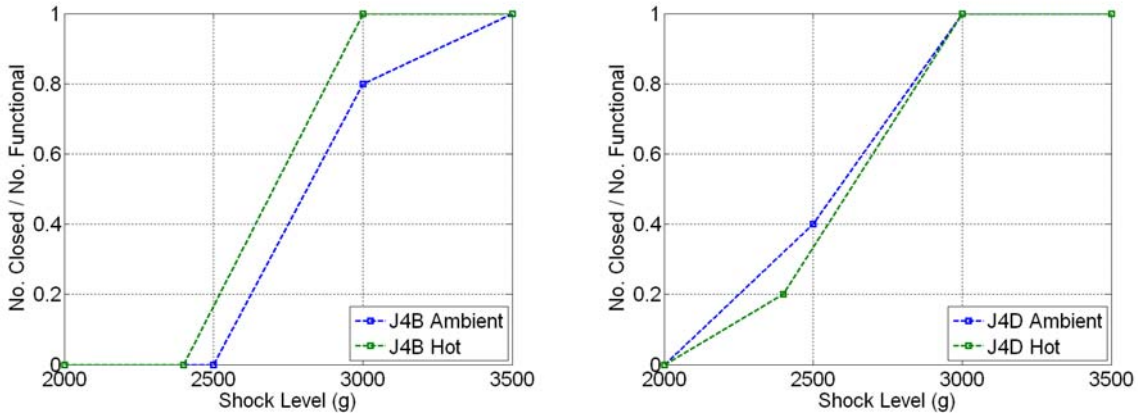

Figure 8. Effect of hot thermal extreme on switch threshold for J4B and J4D.

2.4 Modal Testing

2.4.1 Purpose

The goal of modal testing was to measure as many of the approximate linear resonant frequencies in both open (2nd stable position) and closed (1st stable position) positions of the shock switch as possible. These results were used to validate the mechanical response of the models for revision 4 shock switches. Typically, for linear systems, modal information is used for model validation. Since the shock switches have inherent geometric nonlinearities, the approach needs to be modified slightly. For model validation of the shock switches, modal data collected with very small motions around each of the stable equilibrium points was used. This is similar to standard practice in that modal information is used, but it differs since that data will be available about two stable equilibrium conditions rather than the single stable condition that is typical. Model predictions became available for the in-plane resonances during testing and the most recent model results are used for comparison. No model predictions are available for the out-of-plane resonances.

2.4.2 Test Description

The experimental modal data used for validation of the dynamic models consists of two tests that collectively measure the in-plane and out-of-plane resonant frequencies of the various devices. A commercial laser Doppler vibrometer (LDV) system is used for the out-of-plane measurements, and a high speed camera and feature tracking method is used for in-plane measurements. A test to verify the hypothesis that friction caused revision 2 parts to fail in FY07 was also added to the in-plane modal testing for revision 4 that is the main focus here.

2.4.2.1 Out-of-Plane Test

A Polytec Micro System Analyzer was used to measure the out-of-plane resonant frequencies and mode shapes. Measurements were made on three un-metalized revision 4 dice. A piezo shaker was used to shake the substrate of the dice normal to the parts, and the laser Doppler velocimiters in the Polytec system measured the normal velocity of the substrate and various points on the devices under test. Figure 9 shows the points used on an image of one of the devices tested. The exact locations would differ between devices since device geometry changes, but the general positioning remained the same. Since the mass and springs were completely covered by a Poly4 shadow mask, only the small T-bars on either end of the mass were available for measurements.

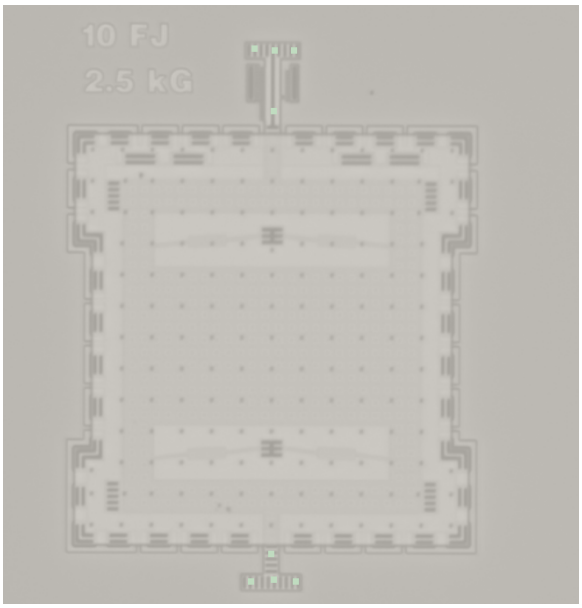

Figure 9. Measurement locations for out-of-plane modal testing.

Each of the devices on the three dice was positioned in the first stable location. Transmissibility from the substrate motion to the device motion in the normal direction was captured with the Polytec. This was repeated with each of the devices in the second stable location. A frequency resolution of 80 Hz was used for the Fast Fourier Transform (FFT) on all results. These results were used to identify the resonant frequencies of the devices as well as the mode shapes corresponding to those frequencies.

2.4.2.2 In-Plane Test

The in-plane resonant frequency results are based on high speed camera movies taken of test structures on revision 2 and revision 4 dice. The revision 4 data was for model validation and the revision 2 data was to verify the hypothesis that frictional forces were the source of revision 2 failures. The revision 4 dice were not metalized. The revision 2 dice were in packages from FY07 testing that had been de-lidded for this test. Each of the test structures was pushed with a probe to the unstable equilibrium point going towards the open stable position and towards the closed stable position. Examples of before and after pictures from this operation for one case are shown in Figure 10. When the spring force overcomes adhesion to the probe tip (and friction for revision 2 parts) the test structure snaps away from the probe and rings down to the stable location. All of the test results were collected at a 7 microsecond frame interval (~142,857 Hz) with a 3 microsecond shutter speed. The high-speed images were analyzed with feature tracking software written in Labview to track the ring-down event.

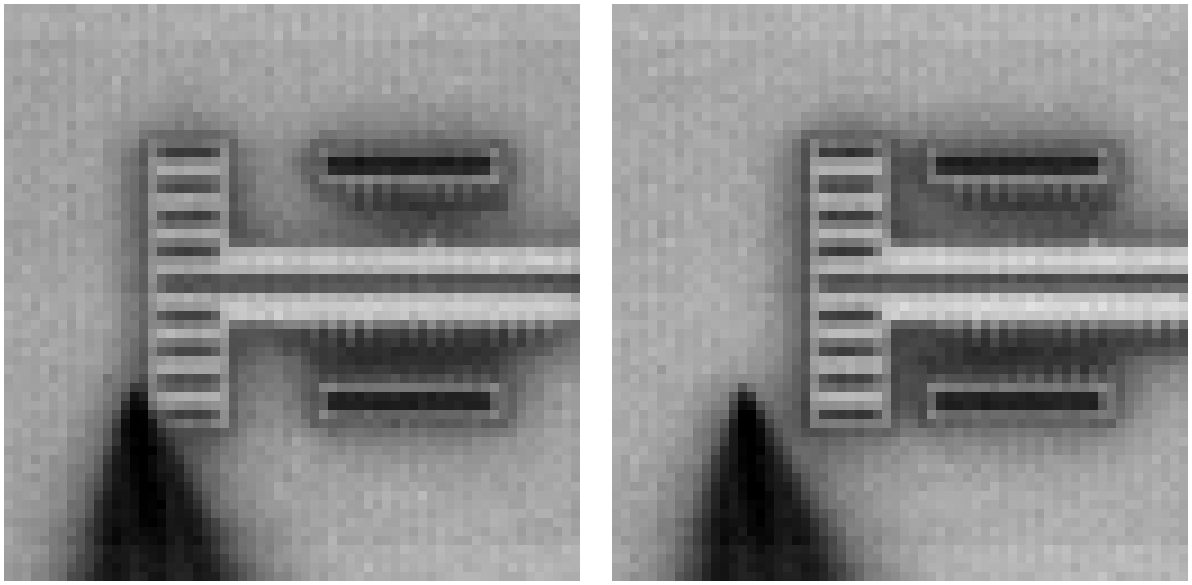

Figure 10. Pictures showing before and after snap through for the closed equilibrium position on one device.

2.4.3 Results

2.4.3.1 Out-of-Plane Results

Table 2 and Table 3 show the measured resonant frequencies for the two most consistent mode shapes identified. The translation normal to the substrate and tilt were the mode shapes most consistently identified. For one device, J4B, the translation mode was more of a tilt with a neutral axis away from the center of gravity (CG) of the device mass.

Table 2. Measured Out-of-Plane Frequencies in Open Stable Location

Device	Die	Translation (Hz)	Tilt (Hz)
J4A-D	1	57890	51950
	2	58280	52580
	3	55230	49920
J4C-D	1	57030	65160
	2	57270	65470
	3	55860	63830
J4B	1	101170**	112110
	2	102270**	113130
	3	NA	NA
J4D	1	148200	76250
	2	149530	76950
	3	145160	74300

Table 3. Measured Out-of-Plane Frequencies in Closed Stable Location

Device	Die	Translation (Hz)	Tilt (Hz)
J4A-D	1	NA	NA
	2	76250	69000
	3	NA	NA
J4C-D	1	71560	81880
	2	71950	82190
	3	70700	NA
J4B	1	125470**	131250
	2	126560**	132500
	3	124220**	129530
J4D	1	176900	91880
	2	NA	NA
	3	174400	90000

**** Note: operational mode shape for this device is slightly modified from translation. See Figure 12.**

Figure 11 shows the typical shape of the two modes used for the tabular results. These are side views of the maximum mode shape amplitude at the measurement locations shown in Figure 9. The black lines show the nominal equilibrium position. In some cases other mode shapes were identified but they were not consistently identified in all parts, so they hold less value for model validation. Figure 12 shows the anomalous first mode for one device.

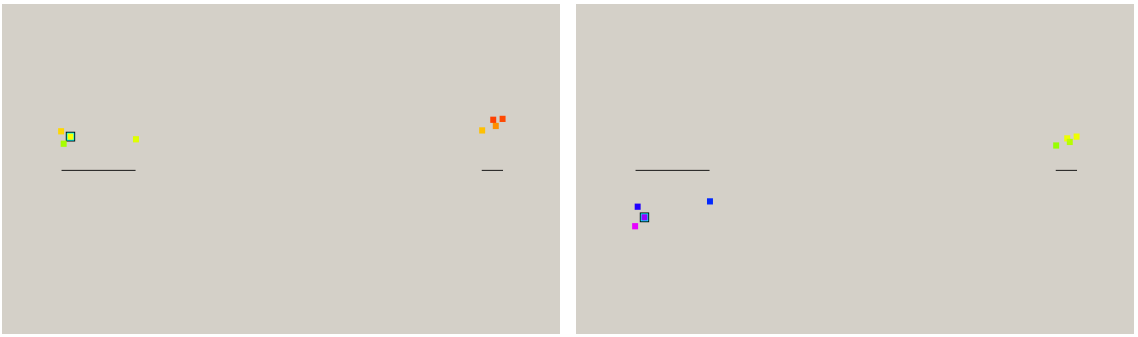

Translation Tilt

Figure 11. Side view of typical operating shapes showing nominal locations (black lines) and measurement location maximum displacement (colored squares).

Figure 12. Side view of first mode for J4B devices. This replaces the first mode (translation) seen in other devices.

2.4.3.2 In-Plane Results

Three main results are presented from this data for the in-plane modal testing. First, the in-plane approximate linear resonant frequencies at the two stable locations for revision 4 shock switches are presented based on FFT analysis of the ring-down events. Second, the ring-down events for revision 2 parts show a significant lack of oscillatory motion as expected from the dimple friction identified as a failure mode in those parts. Third, measurements of the first and second stable locations for the revision 4 devices are documented.

Figure 13 shows an example of the ring-down data collected on revision 4 switches. A short section of the ring down taken after most of the amplitude has died down was used for FFT analysis to determine an approximate linear resonant frequency at each of the stable locations. Table 4 presents the results of this analysis. The error is reported as the readability of the FFT. This obviously does not take into account errors due to nonlinearities still present in the time histories, aliasing, image blurring, or any number of other factors. It is important to note that the sample rate for all of data collected was 142,857 Hz. If the oscillation that was being imaged had a frequency higher than the Nyquist (71428.5 Hz) then the data was aliased and would need to be compensated. Comparison to modeling results helped to identify when this may have occurred and some of the data was corrected for aliasing. Those points that were corrected are identified in the table.

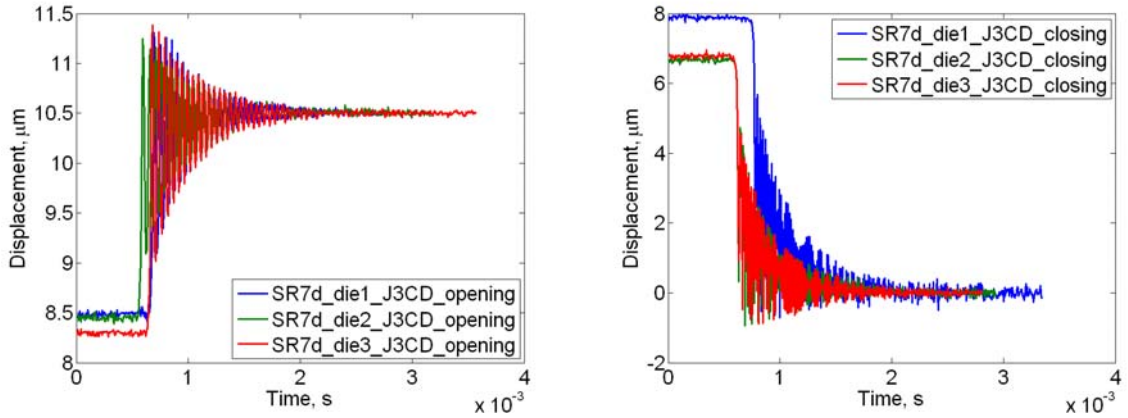

Figure 13. Revision 4: Example of ring-down data collected for one switch type in both directions.

Table 4. In-Plane Modal Results for Revision 4 Shock Switches

Device	Die	Frequency at 1st stable loc (Hz)	Readability (Hz)	Frequency at 2nd stable loc (Hz)	Readability (Hz)
J4A-D	1	54622	1401	12881	1171
	2	57423	1401	18207	1401
	3	53221	1401	16807	1401
J4C-D	1	61624	1401	22408	1401
	2	61624	1401	21008	1401
	3	64425	1401	21008	1401
J4B	1	135785**	1414	43417	1401
	2	135854**	1401	43554	1742
	3	130252**	1401	41811	1742
J4D	1	104395**	2747	45113	1880
	2	104395**	2747	44643	1276
	3	110599**	2304	49020	1401

**These data were corrected for aliasing under the assumption that the frequencies were still below twice the Nyquist frequency.

A comparison to modeled results is shown in Table 5. The average frequency is reported for the measured data with an uncertainty of $\pm 2\sigma$. The modeling results are taken from the FY08 Sandia report on modeling and design [Wittwer et al., 2008b]. These are the most recent model results and they agree very well except in the case of J4D. This is likely because model results do not include error due to edge bias.

Table 5. Revision 4: Comparison of Average Measured Resonant Frequencies to Modeled Results

	Closed Position		Open Position	
Device	**Average Measured (kHz)**	**Modeled (kHz) ±0.02**	**Average Measured (kHz)**	**Modeled (kHz) ±0.02**
J4A-D	55 ± 4	49	16 ± 6	16
J4C-D	63 ± 3	74	21 ± 2	18
J4B	134 ± 6	125	43 ± 2	40
J4D	106 ± 7	167	46 ± 5	57

From ring-down data displacement time histories of revision 2 and revision 4 parts, it is evident that some force is acting on the revision 2 parts that prevents oscillatory ring down in most cases. Figure 14 illustrates this succinctly. This supports the conjecture that there is frictional interference between the dimples used on the devices for off-axis control. There was one case on a revision 2 part where the mass never pulled away from the probe tip. This was on the 10FJ5kG part, package S76, going towards the open stable location.

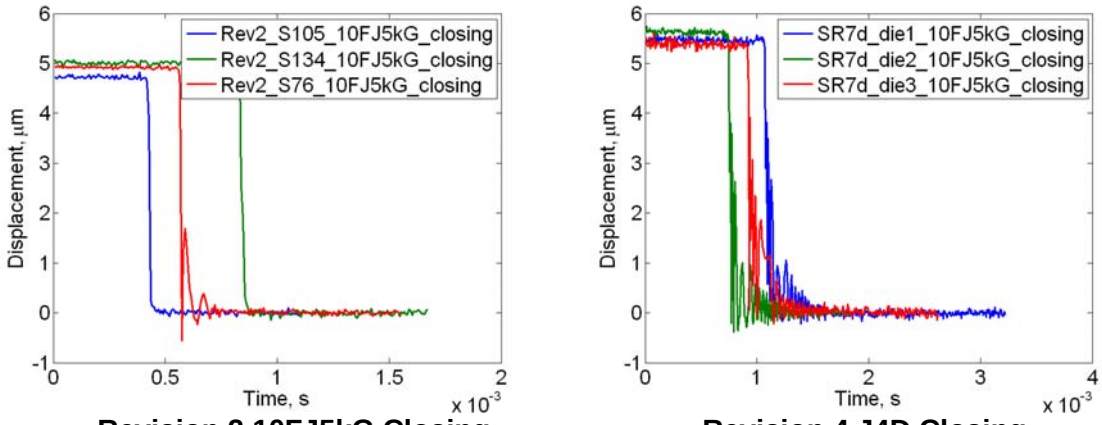

Revision 2 10FJ5kG Closing **Revision 4 J4D Closing**

Figure 14. Comparison of ring down from revision 2 and revision 4 showing significant extra damping in revision 2 nominally due to dimple friction.

Revision 4 stable locations were collected at the same time the ring-down data was collected. The locations measured are shown in Table 6. Stable locations were measured by visual inspection of test devices on the three revision 4 dice. The error on these measurements is +/- 0.125 µm.

Table 6. Stable Locations Measured for Revision 4 Switches

Gel Pack	Device	Die	Closed Stable Loc (µm)	Open Stable Loc (µm)
SR7d	J4C-D	1	0	10.5
		2	0	10.5
		3	0	10.5
	J4A-D	1	0	10
		2	0	10
		3	0	9.5
	J4B	1	destroyed	destroyed
		2	0	8.25
		3	0	8.5
	J4D	1	0	8
		2	0	7.75
		3	0	7.75

2.5 Response to Shock Inputs

2.5.1 Purpose

The purpose of this testing was to record real time switch closure information relative to the shock input. Most of the functional data collected for fully packaged parts was bounding information on switch thresholds, i.e., the switch would stay open at the lower shock level and close at the higher. This only allows for a crude comparison of switch threshold measurements to model results. Real time collection of closure during a shock allows for more refined comparisons with the hope that this will improve modeling further. Only rudimentary comparison to model data was accomplished this fiscal year.

2.5.2 Test Description

A special breakout box (some details in the appendix) was used to record the switch state in real time along with the acceleration from the drop table test. Reinforcing the connection to the packaged part on the drop table was critical for the higher shock levels. The connectors used on the parts were not designed to survive shock environments with the mating connector engaged. Figure 15 shows one instance of this reinforcement. During a 3000 g's drop, there was one case where the connector broke off of the package, destroying it. One packaged part could be tested per drop on the shock machine. This test was combined with the final functionality testing after normal environments so all of the parts used had been exposed to the normal environments. Every time an orientation change was made for the final functional tests, a different part was connected for real time closure recording so that all the data was in-axis.

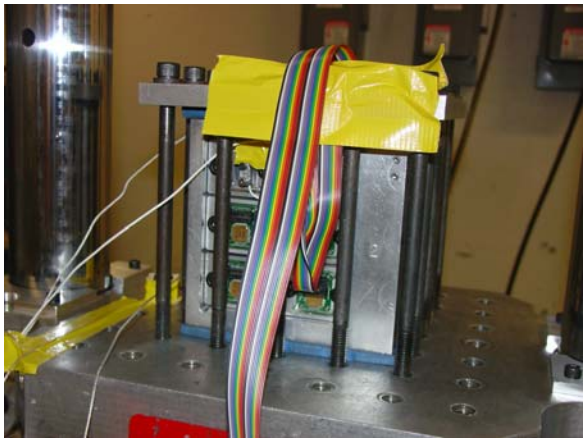

Figure 15. Supporting the cable connection to the packaged part on the drop table to minimize chances of the connector breaking during shocks.

2.5.3 Results

This test was conducted during the last of the functional tests done for the technology readiness series covered later in this report. During each drop for that test, one of the devices being tested was connected to the real-time acquisitions system and time histories were collected indicating exactly when the switch closed during the shock. Figure 16 shows four cases of data collected. In each plot the shock pulse experienced by the switches is plotted along with indications of the switch closure. The intention was that 5.5 V would indicate an open switch and 0.25 V would indicate a closed switch, but there were issues with total power available from the battery used. In practice the switches are open when the voltage indicates > 2 V and the switches are closed when the voltage indicates < 2 V.

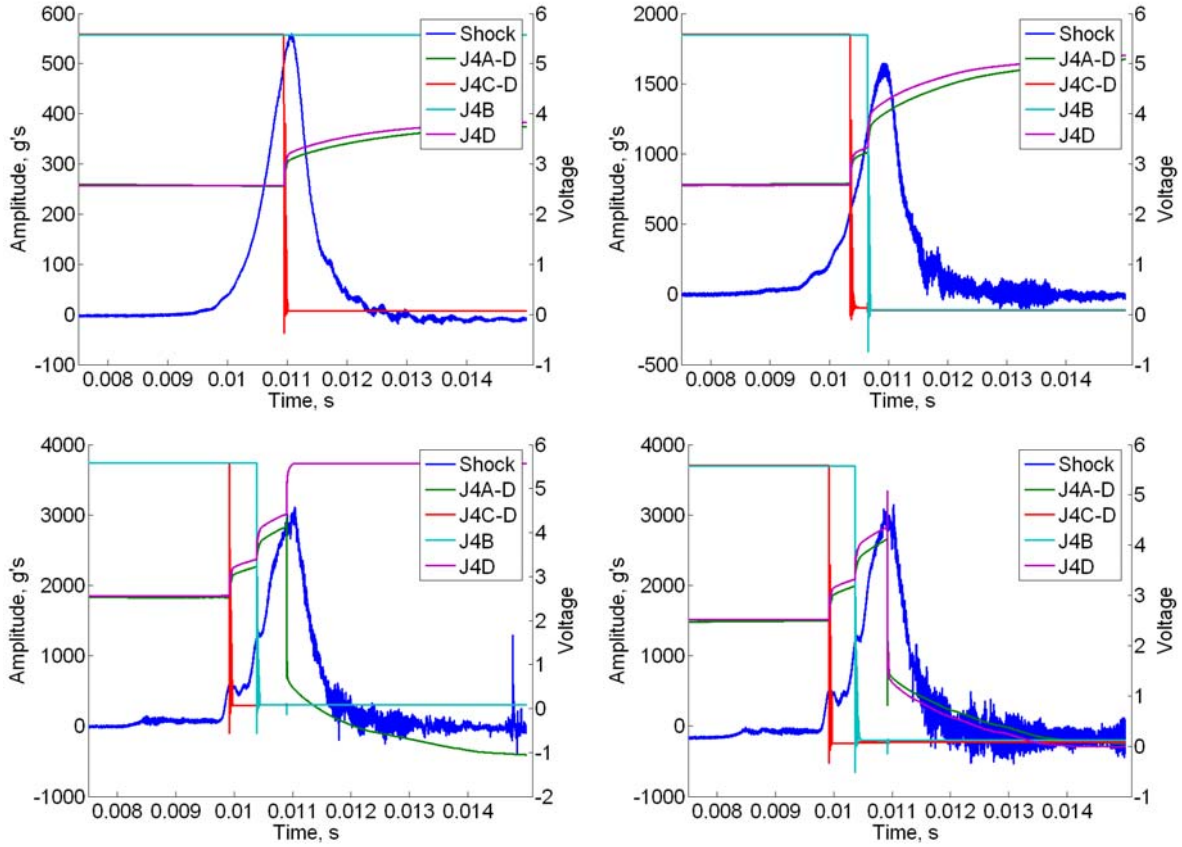

Figure 16. Revision 4: Real-time closure of the shock switches during shock events.

The only comparison to model results accomplished this year was a qualitative comparison to similar figures produced from simulations. Figure 17 shows two examples of model results [Wittwer et al., 2008b] comparing shock input to switch closure events for similar shocks to those in Figure 16. In these figures the switch displacement is indicated rather than a binary open/close as in the measured results. When the switch displacement reaches the contacts (indicated by the blue horizontal line) the switch is considered closed. Qualitatively the responses are similar but more detailed comparison is needed.

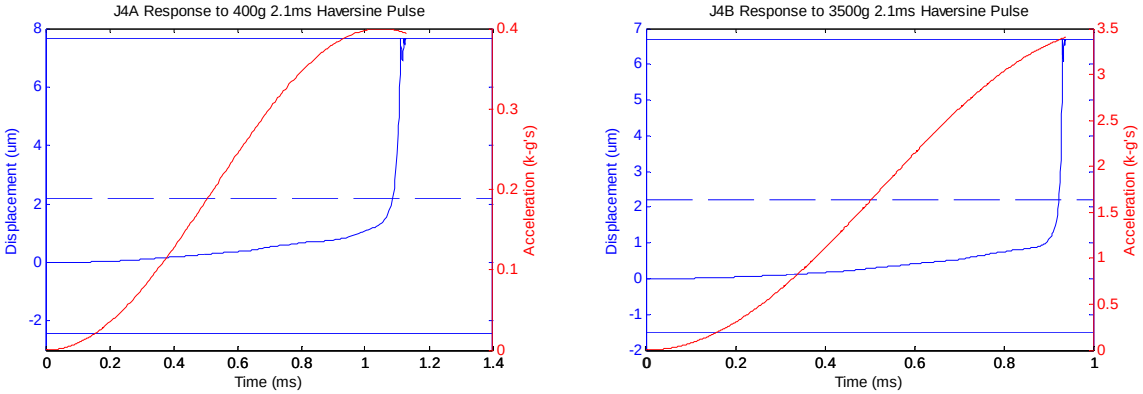

Figure 17. Model results showing switch closure relative to shock inputs.

2.6 Response to Sinusoidal Inputs

2.6.1 Purpose

The goal for testing the sinusoidal response of the shock switches was to validate the modeled response curves. The models predict a frequency dependent threshold for the switches with a minimum threshold very close to the open position resonant frequency. To verify this behavior and validate model results, tests were conducted to measure the switch threshold as a function of frequency for sinusoidal inputs. Measured results show a similar character to model predictions but differences in detail exist. A complete comparison is not possible since the data collected was frequency bandwidth limited.

2.6.2 Test Description

Three revision 4 packages were tested on an electrodynamic shaker. A low mass fixture was used to mount a single packaged part at a time to the shaker (see Figure 18). All efforts were made to minimize the added weight on the shaker armature (which is force limited), assuring maximum acceleration performance of the shaker during testing. One control accelerometer and three auxiliary accelerometers were used to measure the device. The shaker control tuned the shaker so that the response measured at the control accelerometer matched the reference time history.

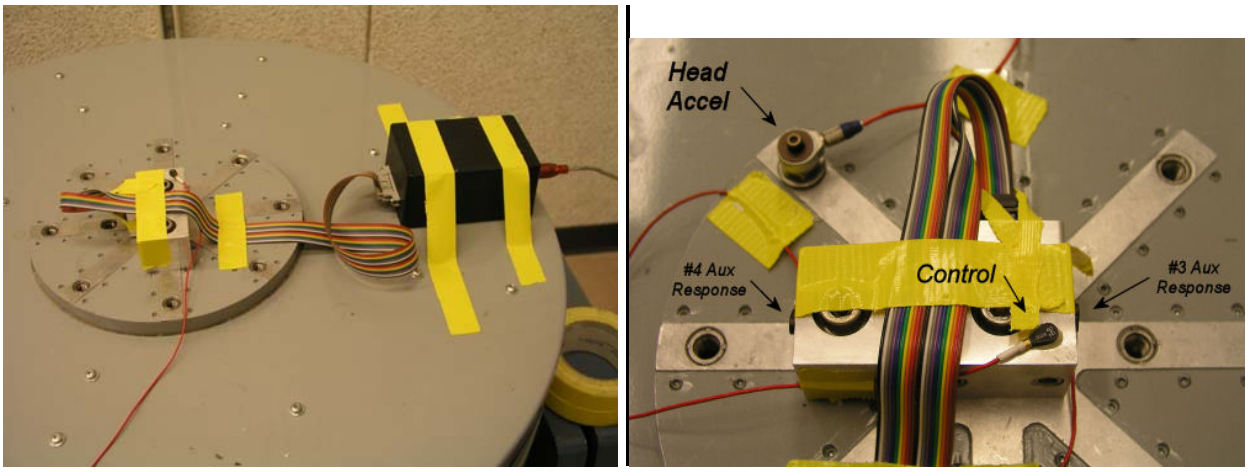

Figure 18. Images of test setup showing test fixture with one package bolted to shaker.

A WAVSYN pulse reference time history was used for all of this testing. That is an impulsive sine wave with a single frequency as shown in Figure 19. Initial tests were done with a continuous sine wave, but the shaker design severely limited the amplitudes attainable with this reference. The impulsive sine wave circumvented those limitations while still producing a sinusoidal shaker motion with only one frequency. Another limitation encountered was the 10 kHz limitation on the shaker control system. Modeling results indicated that tests up to 20 kHz would be needed to fully capture the details desired. Tests were conducted up to the current limit and efforts are in progress to configure a system that will allow testing up to 20 kHz.

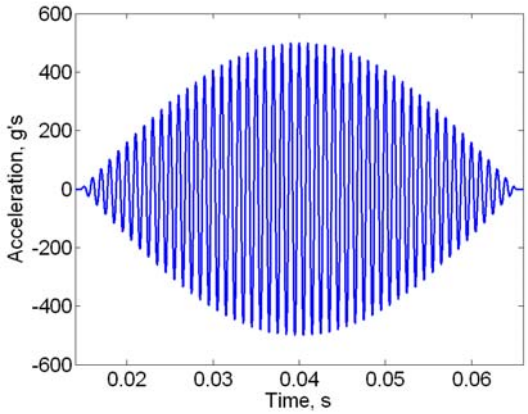

Figure 19. 500 g's 1000 Hz WAVSYN pulse with 101 half sines.

Even with the WAVSYN reference time history, the performance was still limited to a maximum acceleration of approximately 500 g's. This only allowed for testing of the J4A-D switches with a nominal threshold around 400 g's. The reference time history for the shaker level was set to 500 g's, and pulses were specified by indicating the attenuation from that nominal level in dB. Typically, tests would start at -9 dB and the level would be increased in 3 dB increments until the switch closed. Then a self-test would be run to verify that the switch was functional and a manual implementation of the bisection method for the input amplitude would be implemented. This process would stop when the switch threshold was bounded to within 0.2 dB. Two examples of attenuated WAVSYN pulses are shown in Figure 20. Self-tests were conducted after every closure to ensure functionality and to open the switch.

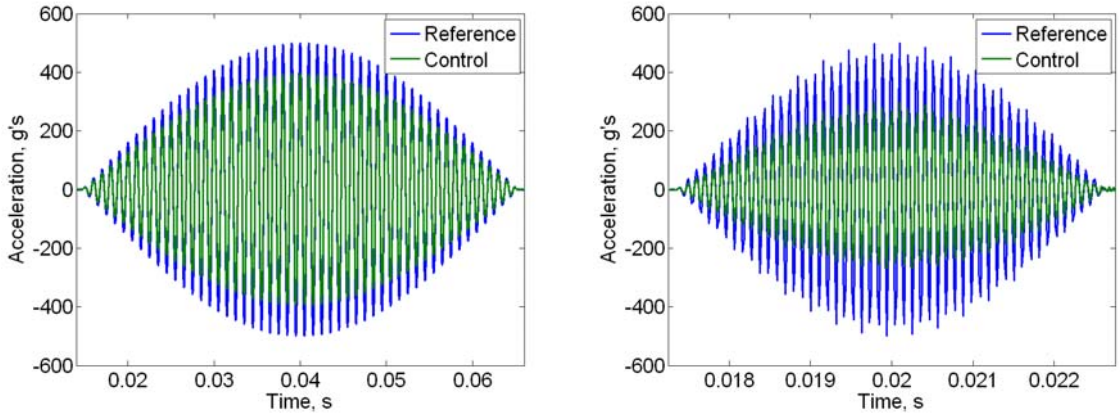

Figure 20. Reference and measured response at control accelerometer for two cases: 1000 Hz at -2 dB and 9600 Hz at -4.9 dB, respectively.

2.6.3 Results

Figure 21 shows the high and low threshold boundaries found for each of the three switches tested. Only the switch J4A was tested on each part. Several interesting observations can be made from this data. First, the low frequency thresholds show a fair amount of variability but the mean value (measurement mean 454 g's, standard deviation 57 g's) matches the model

prediction for the nominal threshold of 405 g's quite well. Second, while the data looks very noisy, it in fact shows a great consistency between parts. All of the peaks and valleys in the plot occur at the same frequencies for all three parts. Last, the overall trend of the threshold is down as frequency increases.

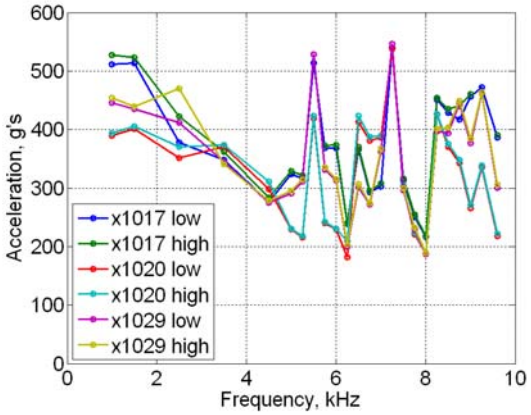

Figure 21. Switch threshold boundaries for J4A-D switch on three devices tested.

Modeling results covered in another report [Wittwer et al., 2008b] show similar character but do not match the specific frequencies for the peaks and valleys. Figure 22 shows one of those results. Since the measured data could not be collected out to 20 kHz full bandwidth, comparisons cannot be made. However, the general character of the response is very similar in both cases.

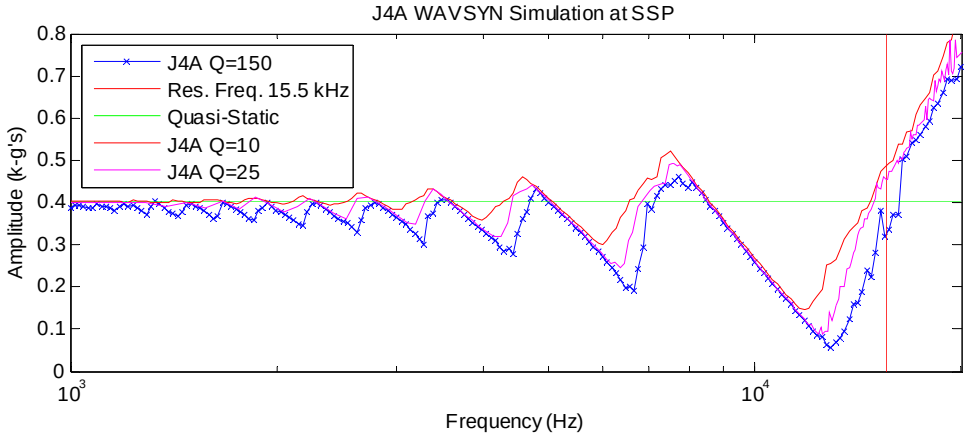

Figure 22. Model results for switch J4A response to WAVSYN inputs.

Work is ongoing to extend the measured data up to 20 kHz. To do this, a new control system needs to be implemented for the shaker that samples at a higher rate, thus allowing for control to a higher frequency.

3. Technology Readiness

A technology evolves and matures through a series of stages. One method that is used at Sandia for defining those stages is the Technology Readiness Level (TRL) [Mitchell and Bailey, 2006], [Mitchell, 2007]. The technology readiness activities reported in this section were aimed at demonstrating the integrated key and supporting elements (sensing, self-test, and packaging) of the Sandia MEMS Passive Shock Sensor under realistic environments based on requirements from a system "representative" of the final application. The specific goal for the technology readiness testing this year was to subject a group of fully packaged parts to normal environments from a "representative" system and verify functionality.

The set of normal environments used are summarized in an internal memo and are based on a combination of a typical system and MIL specs for minimum robustness [Skousen and Cap, 2007]. These consist of thermal, shock, and vibration environments from transportation and flight of a typical system. As a baseline, a functionality check of all the parts was conducted prior to exposure to normal environments. An intermediate functionality check was performed because the schedule for normal environment testing dictated a long break between shock environments and vibration environments. A final functional check was conducted after all normal environment testing. Figure 23 shows a diagram of this flow.

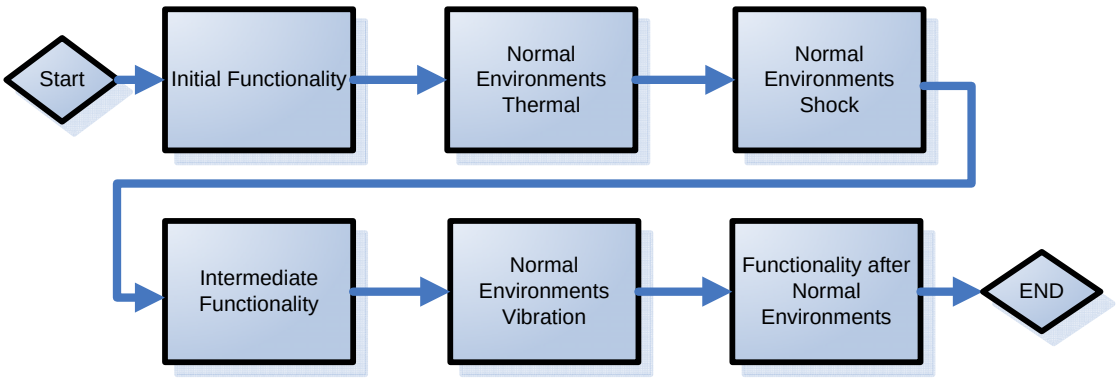

Figure 23. Flow diagram for technology readiness testing.

3.1 Initial Functionality

3.1.1 Purpose

The goal of the pre-normal environment functionality testing was to show that a majority of the devices were functioning as designed before testing their behavior in normal thermal, shock, and vibration environments. The functional tests were performed on a drop table to reach desired

acceleration levels. The outputs of the test were upper and lower acceleration bounds that cause all (of each type) devices to close and remain open, respectively.

3.1.2 Test Description

Twelve fully packaged revision 4 parts were available for the technology readiness testing and these same parts will be used throughout this testing. Another twelve parts were tested for the initial functionality only but held back from normal environment testing. These were all new untested parts that had not been used for any of the other testing in this report. All twenty-four parts were tested for initial functionality on two of the larger test fixtures. Three single-axis accelerometers were fixed to one test fixture to be able to measure the accelerations experienced on each axis. The second test fixture did not have extra accelerometers attached and relied solely on the accelerometer mounted on the carriage. No test variables were changed when changing from test fixture one to two.

A single drop table was used for model validation similarly to the functionality testing covered earlier. The final test configuration from that earlier testing with the 2 ms pulse width and the mechanical isolation was used for all of the technology readiness functionality testing. See Figure 4 for pictures of the setup. The acceleration levels tested were 250 g, 500 g, 750 g, 1000 g, 1500 g, 2000 g, 2500 g, 3000 g, and 3500 g. Levels were chosen so that upper and lower bounds could be determined for each type of device. The upper acceleration bound is defined as the acceleration level at which all devices of a single type close. The lower acceleration bound is defined as the acceleration level at which no devices of a single type close. Two blocks, nine levels, and three axes per level led to a total of 54 drops. Before the first drop, each part underwent a self-test. After each drop, all of the parts on the test block were self-tested again to determine if they closed due to the acceleration of the drop and whether or not they were still mechanically sound.

3.1.3 Results

Figure 24 shows initial functionality test results with from the 24 packaged parts. It displays the ratio of the number of devices that closed to the number of functional devices, defined as those devices that passed the toggling exercise in the self-test, at each test level. These results are very similar to those in Figure 5 from the initial model validation switch threshold testing. The 3500 g levels experienced quite a few failures of J4C-D devices. A bad cable was found to be suspect, and once it was replaced devices appeared to function normally again.

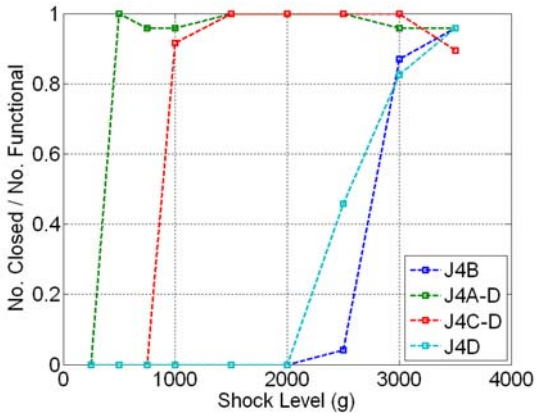

Figure 24. Results from the technology readiness testing initial functionality.

3.2 Normal Environment Thermal Testing

3.2.1 Purpose

The goal of the normal environment thermal testing was to demonstrate that packaged devices could survive and remain functional after exposure to thermal environments. The normal environment thermal test was performed in a thermal chamber normally used for HALT/HASS testing. The output of the test was the number of devices that passed the self-test at the end of the test.

3.2.2 Test Description

The twelve parts on the first of the two test fixtures were tested in the thermal chamber. The parts on test block two were not subjected to the normal environment thermal tests. These parts passed the functionality testing, but were saved in case other parts failed in subsequent tests and replacement parts were needed.

All twelve parts from test block one were put into the thermal chamber at one time (see Figure 25). Sensors were mounted in the chamber to monitor the temperature of the parts. The temperature was ramped up from room temperature to 165°F, where it was held for one hour or until equilibrium was achieved according to the part temperature. At that time, the temperature was ramped down to -65°F and held for one hour or until equilibrium was achieved. This process was repeated 24 times. Then the temperature was brought back to room temperature and allowed to equilibrate. Each ramp in the test had a slope greater than 10°F per minute [Skousen and Cap, 2007].

Before the test, each part underwent a self-test. After the normal environment thermal test, a second self-test was performed to see which devices were still mechanically functioning.

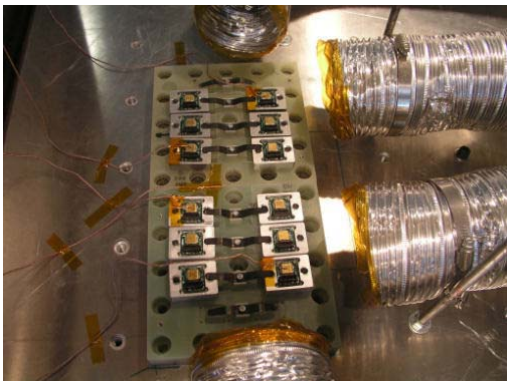

Figure 25. Test parts fixed in thermal chamber.

3.2.3 Results

Figure 26 displays the number of devices that failed the self-test, the number of devices that remained open and the number of devices that spontaneously closed. After experiencing temperature cycles, most switches still passed the self-test when brought back to room temperature. However, a majority of the devices spontaneously closed after the thermal normal environment.

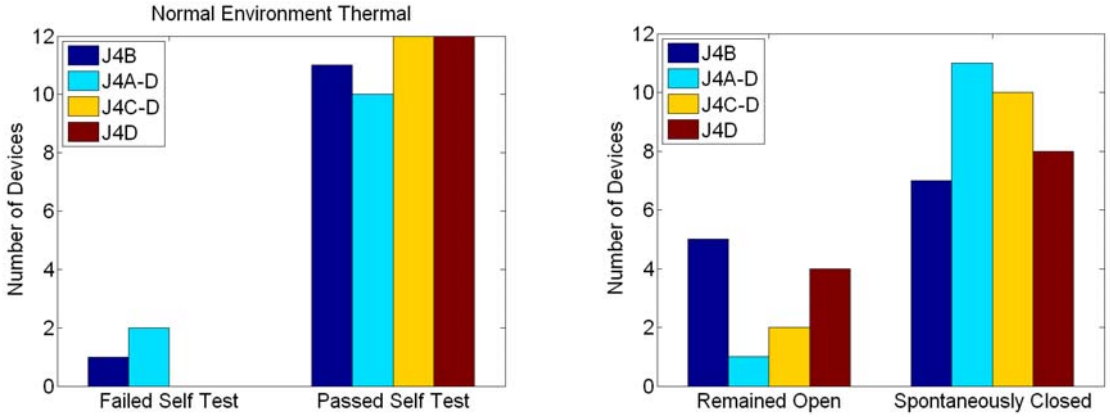

Figure 26. Normal Environment Thermal Test Results

3.3 Normal Environment Shock Testing

3.3.1 Purpose

The goal of normal environment shock testing was to show that after enduring ordinary shock levels, most of the devices were still functioning as designed. The output of the test is the number of devices that pass the self-test after each drop.

3.3.2 Test Description

Twelve parts were tested. The parts were assembled on a single test fixture (test block one) in the same configuration described earlier. Three single axis accelerometers were also affixed to test block one to measure the accelerations experienced in the two off-axes, as well as the acceleration of the test fixture in the direction dropped.

A single drop table was used. Three drops were done in all six axial directions. The first shock aims for an acceleration of 100 g at 5 ms duration. The second drop is a 2000 g shock at 0.3 ms duration. The third shock is 50 g shock at 18 ms duration [Skousen and Cap, 2007]. All of these shocks were applied under ambient temperature conditions.

Before the first drop, each part underwent a self-test. After each drop, all of the parts on the test block were self-tested again to determine if they closed due to the acceleration of the drop and whether or not they were still mechanically sound.

3.3.3 Results

Figure 27, Figure 28, and Figure 29 display the results for the on-axis devices for the normal environment shock testing in both the positive and negative directions. The J4A-D device in one packaged consistently failed the self-test and accounts for all but one of the failures shown. It was stuck in the closed position. This part and one additional package (the only other failure) were removed from the test group for failure analysis [Walraven et al, 2008], and new parts were added to the test group to bring the total back to twelve.

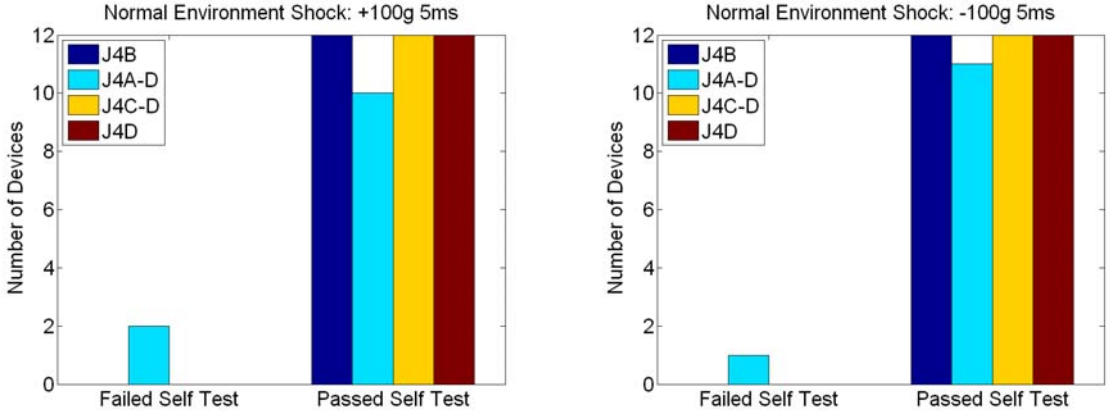

Figure 27. 100 g normal environment shock results.

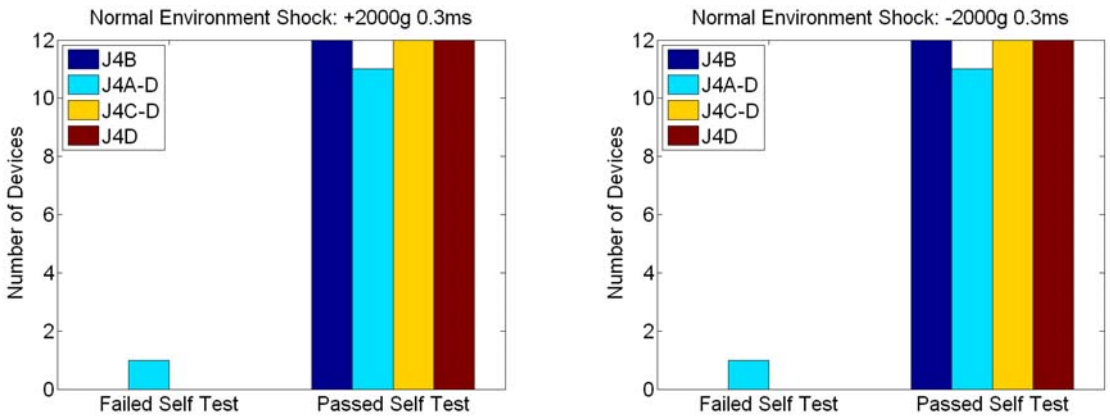

Figure 28. 2000 g normal environment shock results.

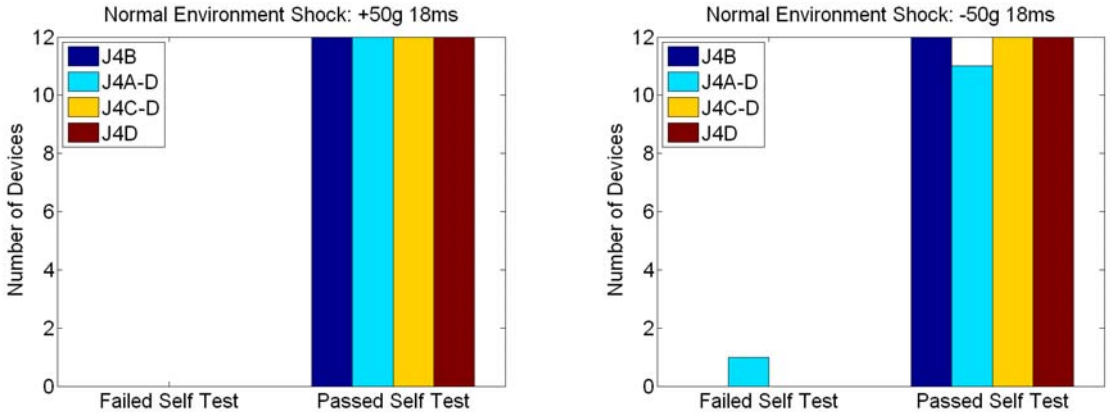

Figure 29. 50 g normal environment shock results.

3.4 Intermediate Functional Testing

3.4.1 Purpose

The goal of the post-thermal and shock normal environment functional testing was to show that a majority of the devices were functioning as designed after enduring normal thermal and shock environments. The intermediate functional tests were performed due to the amount of time between normal environment tests. The functional tests were performed on a drop table to reach desired acceleration levels. The outputs of the test were upper and lower acceleration bounds that caused all (of each type) devices to close and remain open, respectively.

3.4.2 Test Description

The test setup here was exactly the same as for the initial functional testing for technology readiness testing.

The acceleration levels tested were 250 g, 500 g, 1500 g, 2000 g, and 3000 g. Fewer acceleration levels were used in order to quickly establish a general understanding of device performance. One block, five levels, and three axes per level led to a total of 15 drops.

3.4.3 Results

Figure 30 displays the ratio of the number of devices that closed to the number of functional devices, defined as those devices that passed the toggling exercise in the self-test, at each test level. These results are very similar to all previous functionality test results. Results for J4D and J4B were identical and J4D data overlays the J4B results in Figure 30.

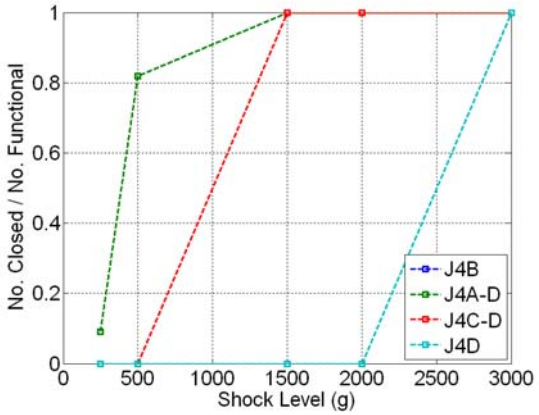

Figure 30. Results from technology readiness testing: intermediate functionality.

3.5 Normal Environment Vibration Testing

3.5.1 Purpose

The goal of the normal environment vibration testing was to show that most of the devices were able to withstand the stated vibrations at temperature and still function. Transportation and flight vibration environments were applied. The output of the test was the number of devices that passed the self-test at the end of the test.

3.5.2 Test Description

Twelve parts were tested. The parts were placed on the test fixture (test block one) that was affixed to the top of a shaker. An insulating cover was placed over the shaker and test parts to control the temperature throughout the test.

A self-test was performed on all of the parts. The parts were heated to 165°F and soaked for one hour on the shaker. A 20-minute sine-on-random test was then followed by a 10-minute random test. This was repeated for each axis, and the parts were allowed to soak for 15 minutes after each axis swap. After the hot test, the parts were self-tested again, then cooled to -65°F, and then

the same test procedure used for the hot test was implemented [Skousen and Cap, 2007]. At the conclusion, the parts were self-tested for a third time.

3.5.3 Results

Results are shown in Figure 31. Device position (open/close) is not reported. Some devices closed during the tests, but no distinction can be made between closures due to temperature sensitivity and closures due to test set up and handling.

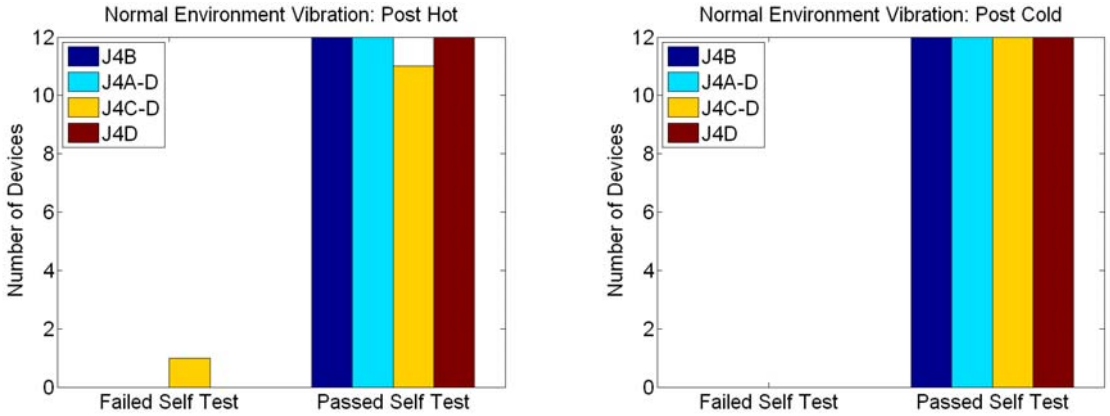

Figure 31. Normal environment vibration test results.

3.6 Final Functional Testing

3.6.1 Purpose

The goal of the final functionality testing was to show that most of the devices were functioning as designed after enduring all the normal environments for transportation and flight. The functional tests were performed on a drop table to reach desired acceleration levels. The outputs of the test were upper and lower acceleration bounds that cause all (of each type) devices to close and remain open, respectively.

3.6.2 Test Description

This test is exactly like the initial and intermediate functionality tests for the technology readiness test series.

3.6.3 Results

Figure 32 displays the ratio of the number of devices that closed to the number of functional devices, defined as those devices that passed the toggling exercise in the self-test, at each test level. Figure 33 compares all of the functional testing for each switch threshold done in FY08. The consistency in this data indicates that the revision 4 parts have stable and consistent functional performance across a large number of parts and after normal environments.

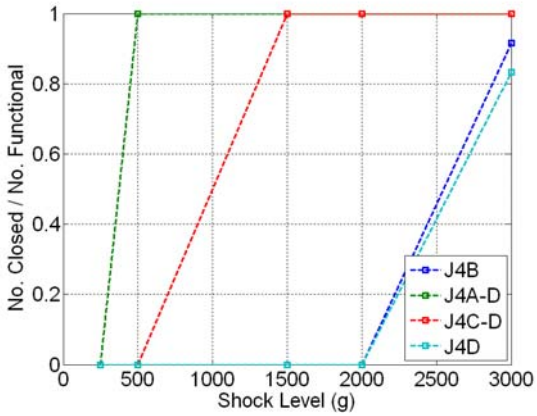

Figure 32. Results from the technology readiness testing final functionality.

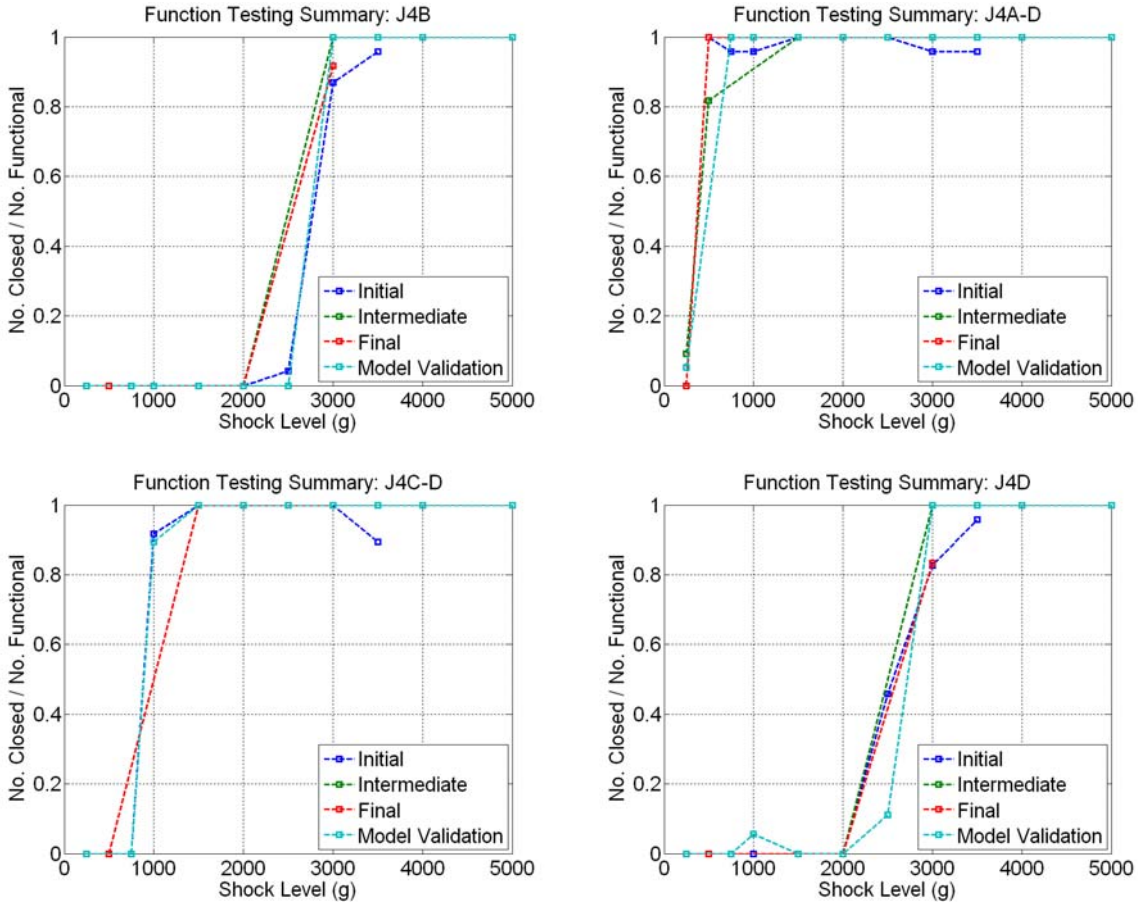

Figure 33. Comparison of all functionality testing in FY08.

4. Conclusions

Revision 4 of the Sandia MEMS Passive Shock Sensor generally functions robustly and with expected performance. The model validation testing activities were used to successfully update some of the models available and proved valuable information for validating the mechanical and thermal modeling activities. The technology readiness testing showed that the switches are robust-to-normal transportation and flight environments. Several issues for future investigation were identified throughout the testing as well. Specific conclusions for the entire test program are collected in the following two sections as well as some description of future work.

4.1 Model Validation

Initial estimates for shock switch thresholds were low compared to measured values. Subsequent modeling efforts improved the model estimated 95% confidence levels so that measured threshold ranges were reasonable. The model estimate for the J4D switch includes a very large range for the 95% confidence level. The switches as-built fall on the edge of this range. Modal test results for the in-plane resonances matched the most recent model results reasonably well except for the J4D switch. This is consistent with the switch threshold results. The only anomaly identified was that the switches seemed to be sensitive to high frequency content in shock inputs. Mechanical filtration of shock inputs was required to complete the testing successfully.

Thermal sensitivity of the bi-stable switch element matched model predictions for all cases except when the switch was fully packaged and potted into the aluminum housing used for the test program. In that case, the switch unexpectedly lost bi-stability at the cold temperature extreme. This issue is being investigated and potentially will lead to new package designs. Verification of the thermal sensitivity of the switch shock threshold was accomplished for the hot thermal extreme and showed little change relative to the resolution of the measurement. The variation that was shown was inconsistent between the J4B and J4D switches. This matches the model prediction in the sense that there should be little change in the threshold with temperature. However, the inconsistency between switches was not explained. Hardware limitations made shock testing at the cold thermal extreme impossible within the timeframe available.

The measurements for real-time shock inputs and sinusoidal inputs match the character of the model results but further comparisons are needed. The sinusoidal response supported the model results in showing that the switches have a frequency dependent shock threshold. Work is in progress to extend the measurements of sinusoidal response to the full bandwidth desired. Designers are working on two methods for reducing the frequency dependence of the shock threshold, mechanical filtering, and design modification. Both options will require test validation in the future.

4.2 Technology Readiness

Functionality of revision 4 of the Sandia MEMS Passive Shock Sensor has been demonstrated by successful testing of 38 packaged units between the model validation and technology readiness testing. From this batch of packages, very few test failures occurred during initial functional testing.

After initial functionality testing twelve packaged parts were subjected to thermal, shock, and vibration normal environments based on a "representative" system. Only the switch health, indicated by the self-test was verified on most tests. The one anomaly noted was that the vast majority of the switches spontaneously closed during the thermal normal environment testing. That was also where the largest number of switch failures occurred. However, additional tests showed that spontaneous switch closures in low temperature environments are likely related to the integration of the LCC into the aluminum housing and subsequent potting (see Section 2.2 of this report). This integration level packaging was developed to facilitate functionality testing, but it highlights an important packaging detail that must not be overlooked in a final packaging design.

Of the 48 switches under test (12 parts with 4 switches each) only 3 failed the self-test consistently after the thermal environment.

The retesting of the shock threshold after normal environments indicated that there was little or no change in the threshold due to normal environments.

5. References

Baker, M.S., C. Gustafson, M. Girardi, R.W. Schroeder, R.L. Hamm, B.D. Young, R.J. Brown, J.T. Slanina, F. Olivas, J.R. Dokos, R.C. Clemens, J.A. Mitchell, M.R. Brake, J.W. Wittwer, D.S. Epp, J.A. Walraven, *The Sandia MEMS Passive Shock Sensor: FY08 Packaging*, SAND2008-5967, Sandia National Laboratories, Albuquerque, NM, 2008.

Mitchell, J.A., *Measuring the Maturity of a Technology: Guidance on Assigning a TRL*, SAND2007-6733, Sandia National Laboratories, Albuquerque, NM, October 2007.

Mitchell, J.A., and B.R. Bailey, *On the Integration of Technology Readiness Levels at Sandia National Laboratories*, SAND2006-5754, Sandia National Laboratories, Albuquerque, NM, September 2006.

Mitchell, J.A., M.S. Baker, J. Blecke, R.C. Clemens, D.A. Crowson, D.S. Epp, J.E. Houston, J.A. Walraven, J.W. Wittwer, *The Sandia MEMS Passive Shock Sensor: FY07 Maturation Activities*, SAND2008-5184, Sandia National Laboratories, Albuquerque, NM, 2008.

Mitchell, J.A., J.W. Wittwer, M.S. Baker, N. Spencer, K.P. Pohl, R.C. Clemens, D.S. Epp, J.C. Gilkey, L.M. Phinney, W. Wilbanks, W.Y. Lu, *On the Design, Packaging and Testing of Micro- and Meso-scale Inertial G-Relays*, SAND2006-5806. Sandia National Laboratories, Albuquerque, NM, 2006.

Skousen, T. J., and J. S. Cap, *Mechanical Shock, Vibration, and Temperature Requirements for EPP MEMS Device*, Sandia National Laboratories, Internal Memo, February 9, 2007.

Walraven, J.A., M.S. Baker, J.W. Wittwer, D.S. Epp, M.R. Brake, R.C. Clemens, J.A. Mitchell, *The Sandia MEMS Passive Shock Sensor: FY08 Failure Analysis Activities*, SAND2008-5185. Sandia National Laboratories, Albuquerque, NM, 2008.

Wittwer, J.W., M.S. Baker, D.S. Epp, J.A. Mitchell, MEMS Passive Latching Mechanical Shock Sensor, in *Proceedings of the 2008 ASME International Design Engineering Technical Conferences*, DETC2008-49178, August 3-6, 2008. New York City, New York, 2008a.

Wittwer, J.W., M.S. Baker, J.A. Mitchell, D.S. Epp, R.C. Clemens, M.R. Brake, J.A. Walraven, *The Sandia MEMS Passive Shock Sensor: FY08 Design Summary, Sandia Report*, (to be submitted as a SAND report in 2008), Sandia National Laboratories, Albuquerque, NM, 2008b.

Appendix A: Fixturing, Electronics, and Software for Testing

A.1 Fixturing

The main fixture used was a 5.25-inch cube/block. This fixture was used for drop table testing and normal environment vibration testing. The block has three testing surfaces, each surface containing up to six packages. The packages on the test block were tightened to 100 in-lbs to assure they were not released during testing. This fixture is designed to fit the drop tables in the shock lab and the shakers in the vibration lab. A top cover plate was bolted to the mechanical test machines holding the test block in place during each test. The test blocks also have mounting locations for accelerometers on all three axes to measure shock or vibration on the actual fixture. Thermocouples can also be attached to the test fixture to monitor package temperature. Figure A.1 shows a solid model of the fixture on a drop table carriage.

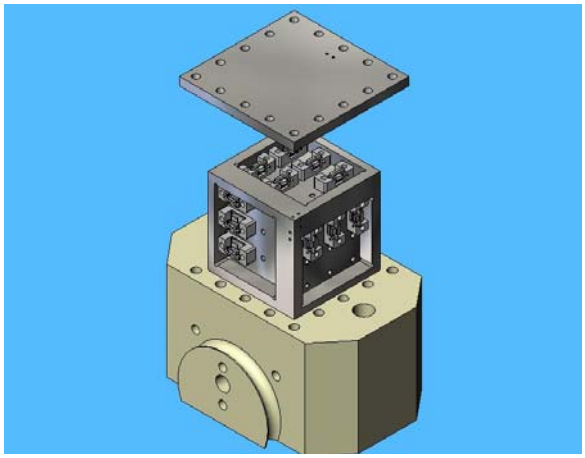

Figure A.1. View of the MEMS unit fixture showing drop table carriage, fixture block, and clamp plate.

A second fixture that was only used for the vibration testing to characterize the response to sinusoidal inputs is much smaller with space for only two packaged parts. It was designed to bolt directly to the armature of the shaker. Figure A.2 shows a diagram of the fixture with two aluminum housings attached in the package part locations. The two large bolt holes in the top are for affixing it to the shaker armature.

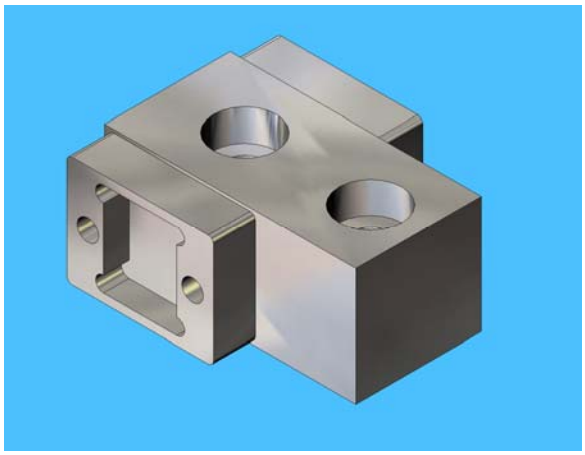

Figure A.2. Smaller fixture for characterizing response to sinusoidal inputs.

A.2 Prototyping Kit

A software program and printed circuit board (PCB) were developed by engineers in SNL/CA to check the state of the switch and apply the self-test at any time in the test series. The software allows one to check the current state of the switch, perform a self-check, and open/close any switch independently. The pause duration for the self-check along with the open/close voltage, open/close current limit, and open/close voltage application time are all adjustable. The software also allows one to save any of the state and self-check data along with a part serial number for data collection. Figure A.3 shows the updated electronics diagram for the FY08 diagnostic system and Figure A.4 shows the diagnostic software interface.

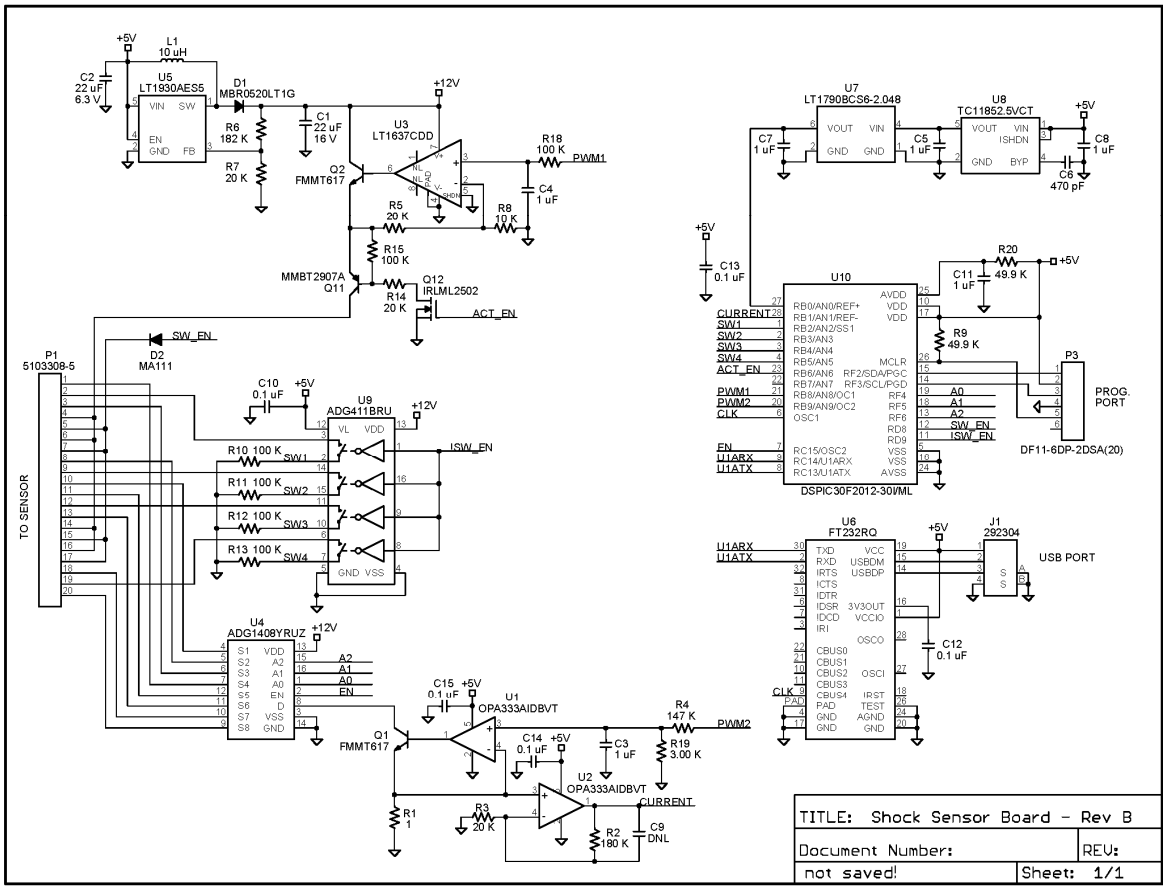

Figure A.3. Schematic of shock sensor diagnostic electronics.

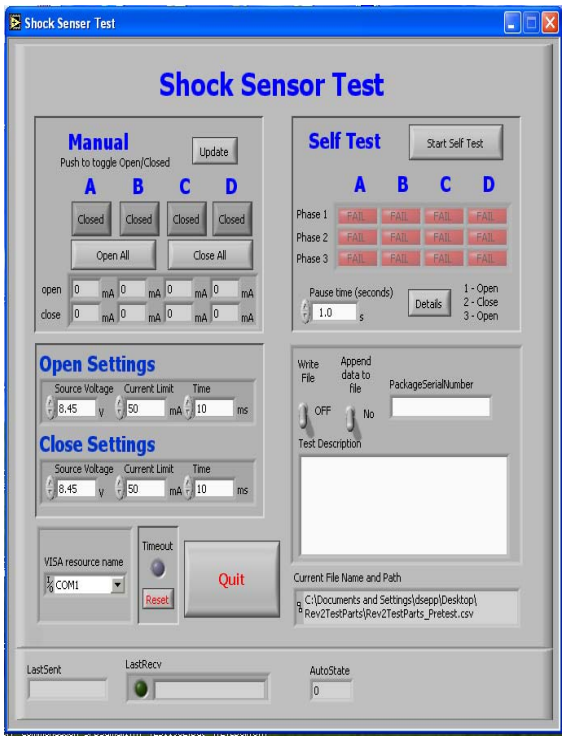

Figure A.4. Screenshot of diagnostic software user Interface.

A.3 Real-Time Electronic Test Box

Collaboration with Ken Pohl resulted in the creation of a test box that can record and indicate closure of the four devices on any one switch at a time (see Figure A.5). There are four light-emitting diodes (LEDs) on the back side of the contraption that are lit when the corresponding device is open. If the device is latched, the corresponding LED is off. Four BNC connections are also available on the top of the device to allow for recording the voltage in the circuits. The output is a TTL signal. High outputs indicate open devices, while low outputs indicate closed devices. In practice the power limitations of the battery reduced the voltage output below TTL levels. For testing, switches were considered open when the voltage was > 2V and closed when < 2V.

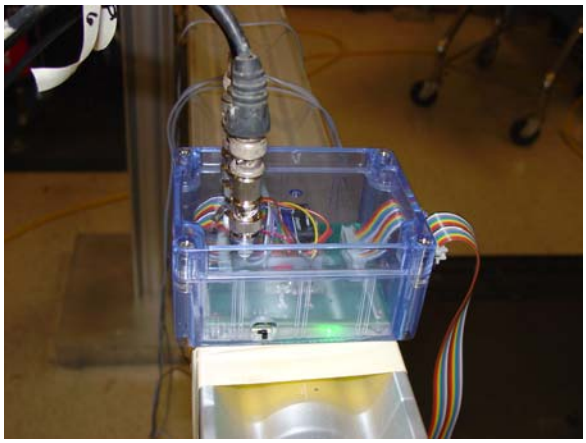

Figure A.5. Real-time electronic test box.

Distribution

1	MS0102	Anna L. Schauer, 2610
1	MS0340	John L. Sichler, 2123
1	MS0340	Steve Harris, 2123
1	MS0344	George Clark, 2626
1	MS0372	James M. Redmond, 1525
1	MS0421	Michael R. Sjulin, 0240
1	MS0427	Robert A. Paulsen, 2011
1	MS0447	Matt Kerschen, 2111
1	MS0530	Hae-Jung L. Murphy, 2623
1	MS0633	Todd Sterk, 2952
1	MS0821	Anthony Thornton, 1530
1	MS0824	Tze Y. Chu, 1500
1	MS0847	Peter J. Wilson, 1520
1	MS1064	Joel B. Wirth, 2614
1	MS1064	Rebecca C. Clemens, 2614
1	MS1064	Ernest J. Garcia, 2614
1	MS1064	Marc A. Polosky, 2614
4	MS1064	John A. Mitchell, 2614
1	MS1069	Mark R. Platzbecker, 1749-1
1	MS1069	Michael S. Baker, 1749-1
1	MS1069	Danelle M. Tanner, 1749-1
1	MS1069	Jonathan W. Wittwer, 1749-1
1	MS1070	Channy C. Wong, 1526
1	MS1070	Jill Blecke, 1526
1	MS1070	David S. Epp, 1526
1	MS1080	Keith Ortiz, 1749
1	MS1081	David J. Stein, 1726
1	MS1081	Jeremy A. Walraven, 1726
1	MS1160	Douglas A. Dederman, 5431
1	MS1415	David R. Sandison, 1110
1	MS1415	Carlos Gutierrez, 1114
1	MS1415	Douglas A. Crowson, 1114
1	MS1415	Jack E. Houston, 1114
1	MS9042	Davina M. Kwon, 8770
1	MS9102	James F. Stamps, 8235
1	MS9102	Paul Y. Yoon, 8235
1	MS9153	Russell G. Miller, 8240
1	MS9154	Janson Wu, 8244
1	MS9154	Jennifer Chan, 8244
1	MS9154	Judy Lau, 8244
1	MS0899	Technical Library, 9536 (electronic copy)


Sandia National Laboratories